Mon. Not. R. Astron. Soc. **261**, 83–102 (1993)

New gas–grain chemical models of quiescent dense interstellar clouds: the effects of H_2 tunnelling reactions and cosmic ray induced desorption

Tatsuhiko I. Hasegawa and Eric Herbst
Department of Physics, The Ohio State University, Columbus, Ohio 43210, USA

Accepted 1992 August 25. Received 1992 August 17; in original form 1992 June 12

ABSTRACT

New models of the chemistry of dense interstellar clouds are presented in which both gas-phase and grain-surface chemistry occur. The dust-grain and gas temperatures are fixed at 10 K and the gas density $n = n(\mathrm{H}) + 2n(\mathrm{H_2})$ remains approximately at 2×10^4 cm^{-3} in these models, in order to represent the chemistry occurring in quiescent clouds. Our previous model has been improved in several substantial ways. The gas-phase network has been extended to 2671 reactions, mainly with the inclusion of recent results involving organo-sulphur reactions. The surface-chemistry network has been extended to 254 reactions. The most significant new surface reactions are exothermic processes of the general type $\mathrm{X} + \mathrm{H_2} \rightarrow \mathrm{XH} + \mathrm{H}$, where X is a molecule, and where a significant activation energy of uncertain magnitude exists. These reactions can occur at appreciable rates due to tunnelling if the activation energy barriers are sufficiently low. If they occur at appreciable rates, the reactions tend to quench complex molecule formation on dust particles. We have also developed simplified rate coefficients to represent cosmic ray induced desorption by impulsive heating of entire grains. Inclusion of this process in our models results in the preferential desorption of selected simple molecules from grain surfaces, but does not allow the desorption of complex organic molecules, which are bound more strongly to grain surfaces. Thus gas-phase observations of many interstellar molecules can still not be accounted for in our models at times later than $\approx 10^6$ yr.

Key words: molecular processes – ISM: clouds – cosmic rays – dust, extinction – ISM: molecules.

1 INTRODUCTION

In response to a growing body of evidence that grain chemistry occurs in the interstellar medium (Williams & Millar 1992), we have recently published models of the chemistry of quiescent dense interstellar clouds in which both grain-surface and gas-phase chemistry are included (Hasegawa, Herbst & Leung 1992, hereafter HHL). Earlier models include those of Pickles & Williams (1977a,b), Allen & Robinson (1977), Tielens & Hagen (1982), d'Hendecourt, Allamandola & Greenberg (1985) and Brown & Charnley (1990). The focus of our models, in which the physical conditions are held fixed at standard dark-cloud values, has been on the formation of organic molecules on dust particles. It was found that organic molecules can grow on grain surfaces as well as in the gas as long as the dominant form of hydrogen is molecular rather than atomic (see also Brown 1990). Atomic hydrogen tends to convert reactive surface radicals, which might otherwise associate to form more complex species, into more stable, hydrogen-containing molecules (HHL). Models in which the initial gaseous abundances consist of purely neutral atomic species were found to lead to little if any complex molecule production on grain surfaces, although gas-phase production of these species followed by accretion occurs. Models in which the so-called 'normal' initial conditions of our previous gas-phase models are utilized, where hydrogen is molecular, were found to lead, on the other hand, to complex molecule production on grain surfaces equally efficient on average to that in the gas phase. At a so-called 'early time' of about $10^{5\text{–}6}$ yr, these latter models also appear to be able to match both observed gas-phase and grain-mantle abundances in quiescent regions.

The models of HHL suffer from some serious defects common to all models in which grain chemistry is included, basically due to the large uncertainties associated with grain

chemistry, and the attendant need to make certain simplifying assumptions. HHL considered only large 'classical' grains and ignored the chemistry occurring on PAHs. They assumed that migration of physisorbed species between lattice adsorption sites on grain surfaces occurs under thermal conditions at 10 K, i.e. non-thermal migration mechanisms were ignored. A consequence of this assumption is that grain chemistry is dominated by reactions involving those reactive species (atoms, radicals) able to migrate rapidly on cold grain surfaces. In particular, atomic H, due to its ability to tunnel from site to site, becomes the most important reactant as long as its surface concentration remains non-negligible. Although H_2 can be a more abundant surface species and also migrates effectively, its reactions have not been considered as fully by HHL and previous authors because they involve activation energy barriers. HHL also assumed that desorption occurs via thermal evaporation only, so that after a sufficient period of time ($\approx 10^7$ yr) the gas phase is totally depleted of neutral molecules containing atoms heavier than hydrogen and helium.

The sensitivity of the HHL model results to some of these assumptions can be tested. In particular, we report in this paper how these model results are affected by changes in the surface chemistry network and by the inclusion of non-thermal desorption. The surface chemistry network has been extended to include, among other new reactions, a significant number of reactions of the type

$$X + H_2 \longrightarrow XH + H \qquad (1)$$

where X is a radical. Despite the existence of activation energy barriers, these reactions can be sufficiently rapid, due to tunnelling processes, to affect the results severely. Their major effect is to disrupt the grain synthesis of complex molecules by converting reactive organic radicals into less reactive H-rich (more 'saturated') forms. Non-thermal desorption via impulsive cosmic ray heating of the entire grains (Léger, Jura & Omont 1985) has been included and found to maintain a sizeable concentration of selected small, but not large, molecules in the gas phase. The result is that, at times significantly later than 'early time' (10^{5-6} yr), complex molecules still do not exist in the gas phase, in agreement with the results of our earlier model.

The remainder of this paper is organized as follows. After a brief discussion of the model in Section 2, we discuss the results when X–H_2 and other new surface reactions are included in Section 3. In Section 4 the derivation of our cosmic ray induced desorption rates is considered, while in Section 5 model results obtained with cosmic ray induced desorption are discussed. Finally, in Section 6, our conclusions are given along with limited comparisons between observational results for quiescent regions and our model calculations.

2 MODEL

The model results have been obtained by solving coupled kinetic differential equations of the type (HHL)

$$\mathrm{d}n(i)/\mathrm{d}t = \sum_l \sum_j K_{lj} n(l) n(j) - n(i) \sum_j K_{ij} n(j) - k_{\mathrm{acc}}(i) n(i) + [k_{\mathrm{evap}}(i) + k_{\mathrm{crd}}(i)] n_{\mathrm{s}}(i), \qquad (2)$$

$$\mathrm{d}n_{\mathrm{s}}(i)/\mathrm{d}t = \sum_l \sum_j k_{lj} n_{\mathrm{s}}(l) n_{\mathrm{s}}(j) - n_{\mathrm{s}}(i) \sum_j K_{ij} n_{\mathrm{s}}(j) + k_{\mathrm{acc}}(i) n(i) - [k_{\mathrm{evap}}(i) + k_{\mathrm{crd}}(i)] n_{\mathrm{s}}(i) \qquad (3)$$

where $n(i)$ and $n_{\mathrm{s}}(i)$ are, respectively, the gas and surface concentration of species i; K_{lj} and k_{lj} are, respectively, the gas phase and surface rate coefficients for reactions between species l and j; $k_{\mathrm{acc}}(i)$ is the grain accretion rate for species i, which includes a sticking coefficient of unity; $k_{\mathrm{evap}}(i)$ is the thermal evaporation rate for species i, and $k_{\mathrm{crd}}(i)$ is the cosmic ray induced non-thermal desorption rate coefficient for species i. All rate coefficients other than those for cosmic ray induced desorption, which are derived in Section 4, have been discussed extensively in HHL. Both gas-phase and surface reactions are assumed to take place at a temperature of 10 K; non-thermal migration of surface species (Brown 1990) is not considered. The elemental abundances used to describe the gas phase + grain mantle are the so-called 'low metal' abundances (Leung, Herbst & Huebner 1984; Graedel, Langer & Frerking 1982). Two sets of initial conditions, in which grain mantles do not yet exist, have been utilized: (1) the gas phase consists entirely of neutral atoms, and (2) the gas phase consists of molecular hydrogen plus atoms in the state of ionization found in diffuse clouds. The latter set of initial conditions is used in our gas-phase models (e.g. Herbst & Leung 1989, 1990) and will be referred to as 'normal'; the former set will be referred to as 'atomic'. The initial gas density is $n = n(\mathrm{H}) + 2n(\mathrm{H_2}) = 2 \times 10^4$ cm^{-3}; because most of the hydrogen remains in the gas phase, n remains constant although, for atomic initial conditions, the dominant form of hydrogen changes.

The gas-phase reaction network of HHL has been improved by the addition of the sulphur chemistry network of Millar & Herbst (1990) which emphasizes organo-sulphur chemistry. With these reactions and several other minor additions, the gas-phase network now consists of 2671 reactions. The surface-reaction network has been redone more thoroughly and now consists of 254 surface reactions, 158 cosmic ray desorption rates, and about a dozen non-zero thermal evaporation terms. Several new species have been added, most importantly C_2H_5CN(H_5C_3N) and HNCO. The major changes to the surface-chemistry network include the following:

(i) hydrogenation of hydrocarbons by H_2 reactions;
(ii) hydrogenation of other species by H_2 reactions;
(iii) reactions involving light radicals, and
(iv) reactions from shock chemistry.

Categories (i) and (ii) are the most important. All new surface reactions in the model are contained in Table 1, which also lists their rate coefficients (cm^3 s^{-1}) and activation energy barriers E_{a}, if any. The surface rate coefficients are determined from migration rates, as discussed in HHL, and are dependent on the overall grain density and grain parameters. Tunnelling is included via the assumption that the potential barriers are rectangular in shape and of length 1 Å (HHL; Tielens & Hagen 1982).

For hydrocarbons with more than one carbon atom, the following surface reactions have been added to the model:

$$C_n + H_2 \longrightarrow C_nH + H, \qquad (4)$$

$$C_nH + H_2 \longrightarrow C_nH_2 + H, \qquad (5)$$

Table 1. New surface reactions.

Reactants		Products		k_{ij} (cm^{+3} s^{-1})	E_a (K)	Ref.
H	HNO	NO	H2	3.68E+05	1.50E+03	IS
H	HCS	H2CS		1.94E+12	0.00E+00	
H	OCN	HNCO		1.94E+12	0.00E+00	AR
H	OCS	CO	HS	1.94E+12	0.00E+00	Mb
H	C2O	HC2O		1.94E+12	0.00E+00	AR
H	C3O	HC3O		1.94E+12	0.00E+00	AR
H	HC2O	CH2CO		1.94E+12	0.00E+00	AR
H	HC3O	H2C3O		1.94E+12	0.00E+00	AR
H	H2O2	O2H	H2	5.16E+04	1.90E+03	Ma
H	CH4	CH3	H2	1.27E-01	5.94E+03	KT
H	C2H6	C2H5	H2	1.44E+00	4.89E+03	BWL
H	CHNH	CH2NH		1.94E+12	0.00E+00	AR
H	CH2N	CH2NH		1.94E+12	0.00E+00	AR
H	CH3N	CH3NH		1.94E+12	0.00E+00	AR
H	CHNH2	CH2NH2		1.94E+12	0.00E+00	AR
H	CH3NH	CH3NH2		1.94E+12	0.00E+00	AR
H	CH2NH2	CH3NH2		1.94E+12	0.00E+00	AR
H	H3C3N	H4C3N		3.19E+07	7.50E+02	
H	H4C3N	H5C3N		1.94E+12	0.00E+00	
H2	CN	HCN	H	1.33E+00	2.07E+03	S
H2	NH2	NH3	H	2.49E-08	6.30E+03	MD
H2	CH2	CH3	H	1.58E-03	3.53E+03	NBS
H2	CH3	CH4	H	1.82E-08	6.44E+03	KT
H2	C2	C2H	H	3.39E-05	4.20E+03	
				1.20E-00	2.10E+03	
H2	C2H	C2H2	H	3.21E-05	4.20E+03	MD
				1.15E-00	2.10E+03	
H2	C3	C3H	H	2.13E-05	4.20E+03	
				8.61E-01	1.20E+03	
H2	C3H	C3H2	H	2.07E-05	4.20E+03	
				8.46E-01	2.10E+03	
H2	C4	C4H	H	1.67E-05	4.20E+03	
				7.26E-01	2.10E+03	
H2	C4H	C4H2	H	1.65E-05	4.20E+03	MD
				7.19E-01	2.10E+03	
H2	C5	C5H	H	1.44E-05	4.20E+03	
				6.55E-01	2.10E+03	
H2	C5H	C5H2	H	1.43E-05	4.20E+03	
				6.50E-01	2.10E+03	
H2	C6	C6H	H	1.31E-05	4.20E+03	
				6.11E-01	2.10E+03	
H2	C6H	C6H2	H	1.30E-05	4.20E+03	
				6.08E-01	2.10E+03	
H2	C7	C7H	H	1.22E-05	4.20E+03	
				5.81E-01	2.10E+03	
H2	C7H	C7H2	H	1.21E-05	4.20E+03	
				5.79E-05	2.10E+03	
H2	C8	C8H	H	1.15E-05	4.20E+03	
				5.59E-01	2.10E+03	
H2	C8H	C8H2	H	1.14E-05	4.20E+03	
				5.58E-01	2.10E+03	
H2	C9	C9H	H	1.11E-05	4.20E+03	
				5.43E-05	2.10E+03	
H2	C9H	C9H2	H	1.10E-05	4.20E+03	
				5.42E-01	2.10E+03	

Table 1 – *continued*

Reactants		Products		k_{ij} (cm^{+3} s^{-1})	E_a (K)	Ref.
C	C4H	C5H		1.86E+03	0.00E+00	
C	C5H	C6H		1.86E+03	0.00E+00	
C	C6H	C7H		1.86E+03	0.00E+00	
C	C7H	C8H		1.86E+03	0.00E+00	
C	C8H	C9H		1.86E+03	0.00E+00	
C	HS	CS	H	1.86E+03	0.00E+00	MD
C	NS	CN	S	1.86E+03	0.00E+00	MD
C	SO	CO	S	1.86E+03	0.00E+00	MD
C	C2O	C3O		1.86E+03	0.00E+00	AR
N	S	NS		1.72E+03	0.00E+00	
N	HS	NS	H	1.72E+03	0.00E+00	MD
N	NS	N2	S	1.73E+03	0.00E+00	Mb
N	CH2	CH2N		1.73E+03	0.00E+00	AR
N	O2H	O2	NH	1.72E+03	0.00E+00	Ma
N	CH3	CH3N		1.72E+03	0.00E+00	AR
O	HS	SO	H	1.61E+03	0.00E+00	MD
O	C2	C2O		1.61E+03	0.00E+00	AR
O	NS	NO	S	1.61E+03	0.00E+00	MD
O	NH2	HNO	H	1.91E+03	0.00E+00	Ma
O	O2H	O2	OH	1.61E+03	0.00E+00	Ma
O	HNO	NO	OH	1.61E+03	0.00E+00	Ma
S	CH	HCS		1.31E+05	0.00E+00	MD
S	NH	NS	H	5.26E+05	0.00E+00	Mb
S	CH3	H2CS	H	2.05E-01	0.00E+00	Mb
CH	NH	CHNH		2.19E+05	0.00E+00	AR
CH	NH	HCN	H	2.19E+05	0.00E+00	
CH	NH	HNC	H	2.19E+05	0.00E+00	
CH	CN	HCCN		1.31E+05	0.00E+00	AR
CH	NO	HCN	O	1.31E+05	0.00E+00	Ma
CH	O2	HCO	O	1.31E+05	0.00E+00	AR
CH	NH2	CHNH2		1.32E+05	0.00E+00	AR
CH	C3H	C4H2		1.31E+05	0.00E+00	
CH	C4H	C5H2		1.31E+05	0.00E+00	
CH	C5H	C6H2		1.31E+05	0.00E+00	
CH	C6H	C7H2		1.31E+05	0.00E+00	
CH	C7H	C8H2		1.31E+05	0.00E+00	
CH	C8H	C9H2		1.31E+05	0.00E+00	
CH	C2H3	C3H4		1.31E+05	0.00E+00	AR
NH	NH	N2H2		5.26E+05	0.00E+00	AR
NH	CH2	CH2NH		5.26E+05	0.00E+00	AR
NH	CH3	CH3NH		5.26E+05	0.00E+00	AR
OH	CO	CO2	H	1.02E-12	3.00E+02	MD
OH	NH2	NH2OH		3.04E+02	0.00E+00	AR
OH	HCO	HCOOH		1.99E-03	0.00E+00	AR
OH	CH3	CH3OH		4.27E-02	0.00E+00	AR
OH	H2CO	HCO	H2O	1.99E-03	0.00E+00	Ma
CH2	CN	CH2CN		1.71E+01	0.00E+00	AR
CH2	NH2	CH2NH2		3.21E+02	0.00E+00	AR
CH2	HNO	CH3	NO	1.71E+01	0.00E+00	Ma
NH2	CH3	CH3NH2		3.04E+02	0.00E+00	AR
CH3	CN	CH3CN		4.08E-02	0.00E+00	AR
CH3	HNO	CH4	NO	4.08E-02	0.00E+00	Ma
CH3	HCO	CH3CHO		4.08E-02	0.00E+00	AR
CH3	CH2OH	C2H5OH		4.08E-02	0.00E+00	AR
CH3	C3N	CH3C3N		4.08E-02	0.00E+00	
CH3	C5N	CH3C5N		4.08E-02	0.00E+00	
CH3	C7N	CH3C7N		4.08E-02	0.00E+00	
CH4	C2H	C2H2	CH3	2.16E-13	2.50E+02	Ma

References: AR: Allen & Robinson (1977); Ma: Mitchell (1984a); IS: Iglesias & Silk (1978); S: Smith (1988); dH: d'Hendecourt et al. (1985); BWL: Baldwin et al. (1969); MD: Mitchell & Deveau (1983); Mb: Mitchell (1984b); KT: Kurylo & Timmons (1969); NBS: Westley (1980); RefD: Baulch et al. (1984).

where $2 \leq n \leq 9$. The activation energies of these reactions are unknown although limited thermodynamic data suggest that they are exothermic. Based on activation energies of 2100 K for the gas-phase radical H_2 reactions $OH + H_2$ and $CN + H_2$ (Smith 1988), we estimate that a similar activation energy holds for surface reactions of type (4) and (5) since C_n and C_nH are reactive species. However, we have also chosen to run models in which these reactions have activation energies of 4200 K. Even with the lower activation energy, the H atoms produced in reactions (4) and (5) are only a small portion of the overall supply of such surface atoms, which stem mainly from accretion. The reaction between OH and H_2 does produce a significant (1/5–1/6) fraction of the surface H atoms.

The direct formation of C_nH_2 species via association reactions between C_n and H_2 rather than via reactions (4) and (5) is another possibility to be considered. Experience suggests that, if such reactions can occur without large amounts of activation energy, they are likely to form metastable species with structures H_2C_n rather than standard HC_nH acetylenes. However, the lack of theoretical or experimental studies of these systems precludes our using $C_n + H_2$ association reactions in this study. Unless these association reactions are much more rapid than reactions (4) and (5), their inclusion will not affect any of the conclusions obtained here.

Once C_nH_2 species are formed, it is assumed that further hydrogenation via H_2 possesses activation energies too large

for the reactions to be significant. Hydrogenation via H-atom addition does occur, however, albeit with small activation energy barriers (HHL).

The situation when $n=1$ is somewhat different. The reactions

$$C + H_2 \rightarrow CH + H \quad (6)$$

and

$$CH + H_2 \rightarrow CH_2 + H \quad (7)$$

are endothermic, and do not occur at 10 K. The association reaction between C and H_2 is not considered here but could be important. Theoretical studies to determine the potential surface for this reaction are needed. The reaction

$$CH_2 + H_2 \rightarrow CH_3 + H \quad (8)$$

is exothermic and included in the model, but occurs with an activation energy barrier of 3530 K (Westley 1980). The reaction

$$CH_3 + H_2 \rightarrow CH_4 + H \quad (9)$$

is thermoneutral; both forward and backward reactions occur with activation energy barriers ≈ 6000 K (Kurylo & Timmons 1969).

Of the X–H_2 surface reactions in which X is not a hydrocarbon, the most important added to the model is

$$CN + H_2 \rightarrow HCN + H, \quad (10)$$

for which we choose an activation energy of 2070 K based on gas-phase data (Smith 1988). Another surface reaction included,

$$NH_2 + H_2 \rightarrow NH_3 + H, \quad (11)$$

suffers from a large estimated activation energy of 6300 K (Mitchell & Deveau 1983).

The reactions in category (iii) were added because it was found that light radicals, which are thought to be reactive, migrate as rapidly as atoms such as C, N and O, which account for many of the reactions in HHL. Most of the added reactions, involving association of the radicals CH, NH, OH, NH_2, CH_2 and CH_3, were taken from the grain model of Allen & Robinson (1977), although the rate coefficients used have been calculated according to the methods of HHL. In addition, a sample of exothermic reactions mainly without activation energy has been taken from gas-phase shock chemistry models (Mitchell & Deveau 1983; Mitchell 1984a,b); these reactions include those involving sulphur species.

Finally, the surface reaction

$$CO + O \rightarrow CO_2 \quad (12)$$

has been included with an activation energy of 1000 K (d'Hendecourt et al. 1985). In our previous work, this reaction was either included at a rapid rate ($E_a = 0$) or, following Grim & d'Hendecourt (1986), not included at all.

3 RESULTS IN THE ABSENCE OF COSMIC RAY INDUCED DESORPTION

Four model calculations have been run. The models are designated as follows: N(4200K), N(2100K), A(4200K) and A(2100K), where N and A refer, respectively, to 'normal' and 'atomic' initial gas-phase abundances and 4200K and 2100K refer to the assumed activation energy barriers for reactions of type (4) and (5). These models can be compared with Model D (normal initial abundances) and Model B (atomic initial abundances) of HHL.

In Model B of HHL, the initial gaseous atomic hydrogen is converted to mainly gaseous H_2 via surface chemistry in $\approx 10^6$ yr. During this interval, the surface chemistry is dominated by H reactions, leading to the production of saturated species such as H_2O, NH_3, CH_4 and H_2S. Meanwhile, the synthesis of more complex species is occurring in the gas, with peak organic abundances achieved by 3×10^5 yr. Accretion of these species on to grain mantles occurs continuously, where saturation via H reactions ensues. The saturation slows considerably once H_2 is the dominant form of hydrogen, but still occurs. As the gas phase is substantially depleted of its heavy molecules at times $> 10^6$ yr, the organic molecules on the grain surfaces slowly evolve into H-rich (saturated) forms. The surface results of Model B are not in good agreement with limited mantle observations of quiescent regions for times in the range 10^5–10^6 yr, during which the gas-phase results best reproduce observed gaseous molecular abundances (HHL). One particular problem concerns the molecule CO, for which Model B predicts far too low a surface abundance; this molecule is not produced initially on grain surfaces since C and O are more readily hydrogenated. At later times, CO accreting from the gas is still hydrogenated slowly into either H_2CO or CH_3OH.

In Model D of HHL, the initial gaseous abundances are 'normal'. Molecular synthesis occurs readily both in the gas and on grain surfaces; the latter is efficient because of the relative paucity of H atoms to convert reactive radicals into more saturated stable forms. As a result, reactive heavy species are able to associate and produce more complex molecules. By 10^5–10^6 yr, significant abundances of complex molecules have been built up in both the gas and on grain surfaces. At later times, as the gas phase is depleted, the complex molecules residing on the grains are slowly converted to saturated forms. Agreement with limited mantle observations in quiescent sources for times in the range 10^5–10^6 yr is good for the species CO, H_2O, CH_4 and CH_3OH (HHL).

3.1 Comparison between previous and new models

The new models with atomic initial abundances – A(4200K) and A(2100K) – do not differ substantially from the previous Model B of HHL. Essentially, hydrogenation to form more saturated molecules is sufficiently rapid via atomic H processes that the addition of molecular hydrogen hydrogenation reactions of types (4) and (5) is unimportant even if their activation energy is 2100 K.

The surface results of model N(4200K) are very similar to those of the analogous HHL Model D, confirming that, with activation energies of 4200 K, reactions of type (4) and (5) once again are unimportant. Model N(2100K), on the other hand, differs substantially from Model D of HHL. Detailed results of Model N(2100K) are presented in Table 2. In this table, fractional abundances of surface and gaseous species with respect to $n/2$ are listed for times ranging from 10^5–10^7 yr. By the longest time, the gas phase is essentially depleted of heavy neutral molecules.

Table 2. Gas and surface abundances for model N(2100K) expressed as a fraction of total $n(H_2)+0.5n(H)$.

t(yr)	1.0 x 10^5		3.2 x 10^5		1.0 x 10^6		1.0 x 10^7	
Species	Gas	Surface	Gas	Surface	Gas	Surface	Gas	Surface
H	2.0E-04	3.8E-23	1.2E-04	6.3E-24	1.0E-04	2.4E-24	1.2E-04	2.1E-24
HE	2.8E-01	1.5E-21	2.8E-01	1.5E-21	2.8E-01	1.5E-21	2.8E-01	1.5E-21
C	3.7E-05	2.8E-14	1.8E-06	1.1E-18	5.8E-08	5.4E-23	7.7E-18	1.6E-28
N	3.1E-05	1.8E-13	1.5E-05	6.5E-14	1.5E-06	8.1E-16	6.6E-19	2.7E-27
O	1.9E-04	2.7E-13	7.5E-05	4.3E-17	5.9E-06	5.4E-21	1.7E-16	1.2E-29
NA	9.5E-10	1.0E-16	8.7E-10	5.7E-16	5.0E-10	8.4E-16	1.6E-11	3.1E-17
MG	3.9E-09	4.1E-16	3.3E-09	2.1E-15	1.8E-09	3.0E-15	5.0E-11	9.7E-17
SI	1.2E-08	1.2E-15	7.5E-09	4.4E-15	1.4E-09	2.2E-15	1.2E-15	2.2E-21
S	7.8E-08	1.4E-15	6.4E-08	5.6E-13	2.0E-08	1.9E-13	8.2E-13	1.4E-18
FE	1.1E-09	7.3E-17	8.5E-10	3.5E-16	4.0E-10	4.3E-16	2.4E-11	3.0E-17
H2	1.0E+00	4.0E-06	1.0E+00	4.0E-06	1.0E+00	4.0E-06	1.0E+00	4.0E-06
CH	4.2E-09	2.4E-18	9.5E-10	7.1E-24	1.1E-09	1.4E-26	4.3E-18	3.9E-33
NH	4.9E-10	5.3E-17	1.6E-10	2.7E-18	1.1E-10	6.6E-17	2.9E-24	1.4E-26
OH	2.1E-08	1.8E-16	3.5E-08	1.0E-16	1.2E-07	8.5E-18	3.2E-17	7.5E-20
C2	2.5E-08	3.4E-19	1.0E-08	1.7E-20	1.5E-08	2.4E-20	4.7E-28	7.5E-40
NAH	2.3E-13	1.6E-10	1.3E-13	6.8E-10	4.7E-14	1.8E-09	2.9E-16	3.6E-09
MGH	8.3E-13	4.1E-16	1.8E-13	2.1E-15	2.0E-14	3.0E-15	4.2E-19	9.7E-17
FEH	0.0E+00	1.1E-10	0.0E+00	4.6E-10	0.0E+00	1.1E-09	0.0E+00	2.1E-09
CN	7.2E-08	1.6E-17	2.2E-08	3.1E-20	3.7E-09	5.1E-21	2.3E-30	4.1E-32
N2	3.1E-08	4.6E-07	1.3E-07	3.0E-06	1.2E-07	3.9E-06	2.1E-28	3.9E-11
CO	6.7E-05	2.5E-06	6.0E-05	8.9E-06	1.3E-05	8.3E-06	2.6E-25	1.7E-17
SIH	2.8E-11	1.2E-15	1.2E-10	4.5E-15	2.6E-10	2.5E-15	9.5E-17	2.4E-21
NO	6.4E-09	3.2E-12	2.7E-08	6.9E-12	2.9E-08	2.5E-13	3.2E-32	1.6E-14
O2	1.2E-06	2.3E-12	5.0E-06	9.6E-09	3.8E-06	6.4E-06	4.5E-28	1.4E-10
HS	2.3E-11	5.8E-16	5.5E-11	5.8E-14	2.8E-11	5.6E-13	2.6E-18	7.0E-13
SIC	2.8E-11	2.5E-11	9.5E-12	3.3E-11	5.2E-12	4.2E-11	4.3E-27	4.5E-11
SIO	5.2E-10	1.5E-10	2.7E-10	3.0E-10	2.3E-11	4.3E-10	1.5E-26	4.4E-10
CS	6.8E-09	3.3E-16	3.1E-09	2.8E-13	5.1E-10	1.4E-10	5.0E-21	5.0E-20
NS	1.3E-10	8.5E-16	7.0E-11	6.3E-13	2.4E-12	5.6E-12	7.0E-34	7.3E-13
SO	1.1E-09	1.8E-15	9.0E-10	6.7E-13	1.1E-10	6.9E-11	1.6E-27	4.5E-11
SIS	1.2E-11	2.0E-12	6.2E-12	5.3E-12	7.1E-14	6.8E-12	5.2E-23	6.8E-12
S2	7.5E-17	4.0E-18	1.3E-15	1.8E-16	1.4E-15	2.5E-15	5.4E-27	2.9E-15
CH2	3.0E-07	4.5E-16	4.8E-08	1.8E-17	5.1E-09	4.9E-20	1.9E-17	1.6E-28
NH2	7.6E-09	7.5E-17	2.6E-09	1.7E-16	3.8E-09	5.6E-15	8.8E-24	1.3E-26
H2O	1.0E-06	5.0E-05	3.5E-07	1.1E-04	1.7E-07	1.7E-04	3.7E-17	2.0E-04
SIH2	0.0E+00	1.2E-15	0.0E+00	4.5E-15	0.0E+00	2.5E-15	0.0E+00	2.4E-21
MGH2	0.0E+00	6.5E-10	0.0E+00	2.7E-09	0.0E+00	6.8E-09	0.0E+00	1.3E-08
C2H	6.2E-08	4.5E-19	8.3E-09	3.1E-20	3.0E-09	3.0E-20	4.1E-29	8.5E-40
N2H	0.0E+00	4.3E-11	0.0E+00	1.5E-10	0.0E+00	3.7E-10	0.0E+00	5.5E-10
O2H	0.0E+00	9.4E-17	0.0E+00	9.2E-16	0.0E+00	4.9E-12	0.0E+00	1.2E-14
HS2	9.0E-14	6.4E-15	3.1E-13	7.2E-14	1.3E-13	3.6E-13	1.4E-26	4.0E-13
HCN	8.3E-08	4.2E-06	5.5E-09	5.9E-06	1.1E-09	5.9E-06	7.7E-31	5.9E-06
HNC	4.1E-08	2.6E-07	3.2E-09	2.8E-07	1.0E-09	2.8E-07	7.4E-31	2.8E-07
HCO	2.2E-09	6.3E-13	6.8E-10	1.5E-11	4.5E-10	1.5E-11	3.8E-30	1.5E-12
HOC	0.0E+00	4.2E-12	0.0E+00	1.5E-11	0.0E+00	1.4E-11	0.0E+00	2.8E-23
HCS	0.0E+00	6.1E-18	0.0E+00	9.0E-19	0.0E+00	4.3E-16	0.0E+00	1.5E-25
HNO	2.4E-11	5.7E-13	2.4E-12	1.2E-09	1.5E-13	6.2E-08	3.7E-39	8.7E-08
H2S	5.0E-11	7.3E-11	9.3E-11	2.3E-09	7.1E-11	6.6E-08	5.9E-18	8.7E-08
C3	2.0E-08	3.6E-20	7.8E-09	1.4E-20	1.6E-08	2.9E-20	1.1E-33	2.1E-45
O3	0.0E+00	6.8E-08	0.0E+00	2.7E-07	0.0E+00	6.1E-08	0.0E+00	3.4E-21
C2N	2.5E-08	1.2E-15	5.6E-09	2.9E-15	7.2E-11	9.5E-17	3.4E-43	3.0E-45
C2O	0.0E+00	1.2E-18	0.0E+00	9.3E-23	0.0E+00	4.4E-26	0.0E+00	3.6E-54
C2S	9.8E-10	9.7E-17	3.7E-10	7.5E-13	1.6E-11	9.0E-11	4.2E-35	9.7E-11
NAOH	4.1E-14	6.4E-15	4.7E-15	1.2E-14	6.5E-16	1.5E-14	1.3E-28	1.5E-14
OCN	1.6E-09	1.3E-12	1.3E-09	1.8E-15	1.5E-10	1.8E-16	6.4E-54	1.2E-27
CO2	2.6E-07	8.7E-06	1.9E-07	2.1E-05	4.5E-09	2.1E-05	2.5E-41	2.1E-05
OCS	4.3E-08	4.8E-15	1.7E-08	8.2E-15	5.4E-10	8.3E-16	6.3E-36	2.4E-34
SO2	2.6E-10	2.8E-08	6.6E-11	7.0E-08	2.2E-12	7.1E-08	4.1E-39	7.1E-08
CH3	4.9E-09	3.3E-15	5.6E-09	3.1E-15	3.0E-08	1.3E-16	3.4E-17	2.8E-22
NH3	1.4E-08	7.2E-09	3.5E-09	1.2E-08	4.5E-09	2.3E-08	5.2E-24	4.7E-08
SIH3	0.0E+00	1.2E-15	0.0E+00	4.5E-15	0.0E+00	2.5E-15	0.0E+00	2.4E-21
C2H2	2.6E-07	7.0E-08	1.5E-07	7.0E-08	3.7E-08	8.5E-08	1.4E-28	4.7E-12
N2H2	0.0E+00	1.1E-06	0.0E+00	3.9E-06	0.0E+00	9.7E-06	0.0E+00	1.5E-05
H2O2	0.0E+00	3.3E-10	0.0E+00	2.5E-10	0.0E+00	2.0E-06	0.0E+00	4.3E-07
H2S2	4.0E-16	2.0E-17	7.2E-15	9.7E-16	7.8E-15	1.4E-14	1.1E-27	1.7E-14
CH2N	0.0E+00	1.9E-15	0.0E+00	1.6E-16	0.0E+00	1.5E-20	0.0E+00	1.8E-40
CHNH	0.0E+00	3.7E-19	0.0E+00	3.4E-25	0.0E+00	4.2E-26	0.0E+00	2.9E-42
H2CO	1.8E-07	3.2E-06	3.9E-08	6.9E-06	7.7E-09	3.2E-05	5.0E-30	4.2E-05
CHOH	0.0E+00	4.2E-12	0.0E+00	1.5E-11	0.0E+00	1.4E-11	0.0E+00	2.8E-23
HCCN	0.0E+00	1.2E-15	0.0E+00	2.9E-15	0.0E+00	9.5E-17	0.0E+00	3.0E-45
HC2O	0.0E+00	1.2E-18	0.0E+00	9.3E-23	0.0E+00	4.4E-26	0.0E+00	3.6E-54
HNCO	0.0E+00	4.0E-06	0.0E+00	7.2E-06	0.0E+00	7.2E-06	0.0E+00	7.2E-06
C3H	3.9E-08	1.1E-19	5.4E-09	2.4E-20	1.2E-09	3.1E-20	9.1E-35	2.3E-45
H2CS	9.2E-10	3.6E-10	3.0E-10	5.8E-10	9.7E-12	1.0E-09	1.6E-24	1.3E-09
C4	1.7E-08	3.2E-20	5.3E-09	1.0E-20	1.1E-08	2.0E-20	9.5E-43	1.8E-54
C3N	2.2E-08	2.5E-15	5.4E-09	2.4E-15	2.8E-10	3.2E-16	9.8E-31	1.3E-36
C3O	3.0E-11	3.2E-18	5.2E-11	2.3E-17	3.7E-12	4.1E-18	1.1E-46	1.4E-52
C3S	4.0E-10	2.6E-10	1.3E-10	5.3E-10	5.6E-12	5.8E-10	4.6E-40	5.9E-10
CH4	1.8E-06	6.2E-07	1.3E-06	1.9E-06	1.4E-07	2.7E-06	3.0E-17	3.8E-06
SIH4	0.0E+00	2.9E-09	0.0E+00	7.7E-09	0.0E+00	1.4E-08	0.0E+00	1.6E-08

Table 2 – *continued*

t(yr)	1.0 x 10^5		3.2 x 10^5		1.0 x 10^6		1.0 x 10^7	
Species	Gas	Surface	Gas	Surface	Gas	Surface	Gas	Surface
C2H3	5.3E-08	4.4E-14	1.4E-08	7.6E-14	4.1E-09	8.8E-14	1.1E-29	4.5E-18
CHNH2	0.0E+00	3.2E-19	0.0E+00	1.3E-23	0.0E+00	2.1E-24	0.0E+00	1.7E-42
CH2NH	8.8E-10	3.2E-08	2.6E-11	3.7E-08	5.7E-12	3.7E-08	1.5E-36	3.7E-08
CH3N	0.0E+00	1.4E-14	0.0E+00	2.8E-14	0.0E+00	3.9E-17	0.0E+00	3.2E-34
C3H2	2.4E-08	6.1E-09	7.1E-09	9.2E-09	1.7E-09	1.5E-08	1.6E-34	3.6E-12
CH2CN	2.8E-08	3.5E-15	9.7E-10	3.3E-15	1.2E-11	1.1E-16	3.0E-43	3.1E-45
CH2CO	3.6E-08	5.8E-09	2.9E-09	1.1E-08	5.4E-11	1.2E-08	2.0E-41	1.2E-08
HCOOH	1.0E-09	8.5E-11	1.2E-09	5.2E-10	7.4E-11	1.0E-09	1.1E-42	1.1E-09
CH2OH	0.0E+00	4.2E-12	0.0E+00	1.5E-11	0.0E+00	1.4E-11	0.0E+00	2.8E-23
NH2OH	0.0E+00	2.3E-13	0.0E+00	4.5E-13	0.0E+00	3.1E-12	0.0E+00	5.5E-12
C4H	1.2E-07	2.5E-19	1.0E-08	2.9E-20	1.9E-09	2.4E-20	8.1E-44	2.0E-54
HC3N	5.8E-08	5.2E-09	5.4E-09	7.0E-09	1.8E-10	3.5E-09	6.0E-33	1.6E-13
HC3O	0.0E+00	3.2E-18	0.0E+00	2.3E-17	0.0E+00	4.1E-18	0.0E+00	1.4E-52
C5	8.7E-09	1.6E-20	1.5E-09	2.8E-21	1.9E-09	3.5E-21	3.3E-54	6.1E-66
C4N	2.9E-09	3.1E-10	4.0E-10	7.5E-10	7.9E-12	8.4E-10	3.3E-18	8.4E-10
C4S	1.6E-10	2.7E-11	1.1E-11	4.1E-11	7.2E-13	4.4E-11	4.7E-53	4.4E-11
C2H4	1.2E-09	2.5E-09	7.6E-10	4.1E-09	2.2E-11	4.9E-09	6.6E-31	2.6E-13
CH2NH2	0.0E+00	4.7E-19	0.0E+00	8.1E-20	0.0E+00	1.9E-20	0.0E+00	1.7E-40
CH3NH	0.0E+00	1.5E-14	0.0E+00	2.8E-14	0.0E+00	1.0E-15	0.0E+00	5.0E-31
CH3OH	2.7E-09	1.1E-05	9.6E-11	2.7E-05	7.2E-12	5.2E-05	4.2E-31	6.2E-05
C3H3	1.8E-10	3.6E-14	6.8E-11	8.1E-15	2.0E-12	1.3E-14	5.2E-43	3.2E-18
CH3CN	3.7E-09	6.8E-09	2.1E-11	1.5E-08	7.8E-13	1.7E-08	1.0E-43	1.7E-08
H2C3N	0.0E+00	4.4E-15	0.0E+00	5.9E-15	0.0E+00	2.9E-15	0.0E+00	1.4E-19
H2C3O	0.0E+00	2.9E-11	0.0E+00	4.6E-11	0.0E+00	6.7E-11	0.0E+00	6.9E-11
C4H2	2.0E-08	1.0E-08	3.5E-09	1.1E-08	1.9E-10	1.1E-08	2.2E-46	3.2E-12
C5H	4.2E-09	2.4E-20	1.7E-10	3.2E-21	1.2E-11	3.6E-21	1.6E-57	6.2E-66
C6	3.4E-09	6.1E-21	3.6E-10	6.5E-22	2.2E-10	4.1E-22	3.0E-62	5.5E-74
C5N	2.9E-09	1.7E-16	3.7E-10	1.4E-16	6.5E-12	6.1E-18	2.4E-55	2.7E-61
CH3NH2	6.4E-10	9.2E-08	1.9E-11	1.6E-07	3.8E-12	1.6E-07	8.5E-37	1.6E-07
C2H5	0.0E+00	4.4E-14	0.0E+00	7.4E-14	0.0E+00	8.7E-14	0.0E+00	5.5E-18
C3H4	2.3E-10	2.6E-07	2.5E-10	3.1E-07	4.8E-12	3.2E-07	1.2E-42	3.9E-07
C4H3	0.0E+00	8.7E-15	0.0E+00	9.7E-15	0.0E+00	9.3E-15	0.0E+00	2.7E-18
CH3CHO	1.4E-11	4.7E-12	2.5E-12	3.0E-11	1.9E-13	8.4E-11	7.8E-45	1.1E-10
H3C3N	2.0E-10	2.6E-10	2.0E-11	3.6E-10	4.4E-14	1.9E-10	1.3E-56	8.7E-15
C5H2	4.3E-09	1.1E-09	4.1E-10	1.2E-09	1.2E-11	1.3E-09	2.2E-57	3.3E-13
C6H	2.0E-09	9.8E-21	6.7E-11	7.7E-22	3.5E-12	4.1E-22	2.3E-64	5.6E-74
HC5N	5.1E-09	3.8E-10	1.8E-10	4.3E-10	9.3E-13	1.8E-10	1.1E-57	1.2E-14
C7	1.5E-09	2.7E-21	1.2E-10	2.2E-22	5.6E-11	9.9E-23	1.4E-71	2.4E-83
H4C3N	0.0E+00	4.3E-15	0.0E+00	6.0E-15	0.0E+00	3.1E-15	0.0E+00	1.4E-19
CH3C3N	3.7E-10	4.7E-11	8.4E-12	7.8E-11	3.2E-14	7.9E-11	1.4E-46	7.9E-11
H2C5N	0.0E+00	3.0E-16	0.0E+00	3.5E-16	0.0E+00	1.4E-16	0.0E+00	9.5E-21
C2H6	0.0E+00	4.9E-07	0.0E+00	5.9E-07	0.0E+00	7.1E-07	0.0E+00	9.5E-07
C4H4	0.0E+00	2.4E-08	0.0E+00	4.4E-08	0.0E+00	5.6E-08	0.0E+00	9.9E-08
C5H3	0.0E+00	8.8E-16	0.0E+00	1.0E-15	0.0E+00	1.1E-15	0.0E+00	2.7E-19
C6H2	4.5E-09	5.5E-10	6.8E-10	6.2E-10	3.9E-11	3.8E-10	7.4E-63	6.8E-14
C7H	1.1E-09	4.6E-21	1.8E-11	2.5E-22	7.4E-13	1.0E-22	9.7E-74	2.4E-83
C8	7.8E-10	1.4E-21	4.1E-11	7.0E-23	1.9E-11	3.3E-23	1.3E-81	2.3E-93
C7N	5.4E-10	2.8E-17	2.6E-11	8.1E-18	2.6E-13	2.2E-19	8.1E-71	7.8E-77
CH3OCH3	2.6E-12	2.3E-13	1.4E-14	5.3E-13	1.1E-16	5.3E-13	1.2E-45	5.3E-13
C2H5OH	2.9E-12	1.1E-11	7.4E-13	7.8E-11	8.4E-15	1.3E-10	2.1E-45	1.5E-10
CH3C4H	3.3E-09	2.4E-10	3.8E-10	8.4E-10	6.1E-12	8.9E-10	2.5E-57	9.0E-10
C5H4	0.0E+00	4.2E-09	0.0E+00	6.3E-09	0.0E+00	7.6E-09	0.0E+00	1.2E-08
C6H3	0.0E+00	4.5E-16	0.0E+00	5.0E-16	0.0E+00	3.1E-16	0.0E+00	5.5E-20
C7H2	9.2E-10	2.0E-10	2.8E-11	1.5E-10	9.3E-13	8.1E-11	1.5E-73	1.6E-14
C8H	1.1E-09	3.3E-21	1.4E-11	9.5E-23	6.3E-13	3.4E-23	2.1E-83	2.4E-93
HC7N	1.1E-09	7.1E-11	2.2E-11	6.1E-11	1.7E-13	2.3E-11	1.6E-72	1.9E-15
C9	2.2E-10	3.6E-22	9.7E-12	1.6E-23	3.0E-12	5.0E-24	1.2E-91	2.0-103
H3C5N	0.0E+00	5.1E-10	0.0E+00	1.3E-09	0.0E+00	1.6E-09	0.0E+00	1.8E-09
H5C3N	0.0E+00	7.9E-09	0.0E+00	1.9E-08	0.0E+00	2.6E-08	0.0E+00	3.0E-08
CH3C5N	2.6E-11	2.6E-12	1.2E-13	4.0E-12	1.1E-16	4.0E-12	2.4E-71	4.0E-12
H2C7N	0.0E+00	5.6E-17	0.0E+00	4.8E-17	0.0E+00	1.8E-17	0.0E+00	1.5E-21
C6H4	0.0E+00	1.8E-09	0.0E+00	2.8E-09	0.0E+00	3.4E-09	0.0E+00	4.2E-09
C7H3	0.0E+00	1.6E-16	0.0E+00	1.2E-16	0.0E+00	6.5E-17	0.0E+00	1.3E-20
C8H2	5.5E-10	1.4E-10	4.0E-11	9.9E-11	3.1E-13	4.4E-11	3.8E-85	9.1E-15
C9H	1.4E-10	5.9E-22	9.5E-13	1.8E-23	1.0E-14	5.1E-24	9.7E-94	2.1-103
C9N	6.8E-11	3.2E-18	1.5E-12	4.2E-19	2.7E-15	2.0E-21	2.0E-95	1.7-101
CH3C6H	9.5E-11	6.2E-12	3.4E-12	1.6E-11	1.8E-14	1.7E-11	3.2E-77	1.7E-11
C7H4	0.0E+00	6.6E-10	0.0E+00	9.9E-10	0.0E+00	1.1E-09	0.0E+00	1.3E-09
C8H3	0.0E+00	1.1E-16	0.0E+00	7.8E-17	0.0E+00	3.4E-17	0.0E+00	7.2E-21
C9H2	2.1E-10	2.9E-11	1.9E-12	1.9E-11	1.3E-14	7.7E-12	2.2E-93	1.2E-15
HC9N	1.3E-10	8.2E-12	1.3E-12	6.1E-12	1.6E-15	2.1E-12	4.1E-97	2.0E-16
H3C7N	0.0E+00	9.5E-11	0.0E+00	2.2E-10	0.0E+00	2.7E-10	0.0E+00	2.9E-10
CH3C7N	5.3E-12	4.8E-13	1.3E-14	7.2E-13	1.8E-17	7.2E-13	3.2E-86	7.2E-13
H2C9N	0.0E+00	6.4E-18	0.0E+00	4.8E-18	0.0E+00	1.7E-18	0.0E+00	1.5E-22
C8H4	0.0E+00	3.2E-10	0.0E+00	5.3E-10	0.0E+00	6.1E-10	0.0E+00	6.9E-10
C9H3	0.0E+00	2.2E-17	0.0E+00	1.5E-17	0.0E+00	6.0E-18	0.0E+00	9.3E-22
C9H4	0.0E+00	6.3E-11	0.0E+00	1.1E-10	0.0E+00	1.2E-10	0.0E+00	1.3E-10
H3C9N	0.0E+00	1.1E-11	0.0E+00	2.5E-11	0.0E+00	2.9E-11	0.0E+00	3.1E-11
E	3.6E-08		4.1E-08		5.2E-08		8.7E-07	
H+	3.0E-10		8.4E-10		1.5E-09		8.0E-07	
HE+	6.4E-10		8.3E-10		2.7E-09		1.4E-08	

Table 2 – *continued*

t(yr)	1.0 x 10^5		3.2 x 10^5		1.0 x 10^6		1.0 x 10^7	
Species	Gas	Surface	Gas	Surface	Gas	Surface	Gas	Surface
C+	2.9E-09		8.0E-09		8.4E-09		4.7E-18	
N+	5.6E-12		2.6E-12		4.2E-12		2.3E-26	
O+	2.3E-15		1.4E-14		2.4E-14		1.3E-23	
NA+	2.9E-09		2.4E-09		1.7E-09		4.3E-10	
MG+	9.5E-09		8.0E-09		5.4E-09		7.9E-10	
SI+	1.4E-11		3.6E-11		9.3E-12		1.6E-15	
S+	1.2E-10		5.0E-10		1.1E-10		2.1E-11	
FE+	4.8E-09		4.7E-09		4.5E-09		3.9E-09	
O2+	9.1E-12		1.0E-10		1.2E-10		4.5E-31	
CH+	1.8E-13		1.6E-14		3.0E-15		3.9E-22	
SO+	1.1E-11		2.0E-11		6.7E-12		1.8E-23	
H3+	2.2E-09		4.0E-09		1.9E-08		5.6E-08	
CH2+	2.7E-13		3.9E-14		1.7E-14		7.5E-22	
NH2+	1.9E-14		6.9E-15		1.3E-14		3.7E-27	
HCO+	5.2E-09		8.1E-09		6.4E-09		2.5E-29	
HOC+	5.0E-10		5.8E-10		4.5E-10		2.1E-30	
N2H+	5.6E-13		4.9E-12		2.1E-11		6.7E-33	
C2N+	3.4E-10		6.1E-11		1.1E-11		9.7E-37	
HCS+	2.0E-11		3.8E-11		2.4E-11		7.4E-22	
OCS+	2.0E-10		1.4E-10		5.1E-12		2.4E-34	
H3O+	2.0E-09		1.3E-09		1.1E-09		5.8E-19	
HCO2+	4.5E-12		6.7E-12		7.3E-13		4.5E-45	
H2CN+	4.1E-10		5.6E-11		3.3E-11		3.3E-33	
CH3+	3.4E-10		7.0E-11		2.9E-11		3.8E-19	
NH3+	1.5E-12		6.5E-13		1.6E-12		1.1E-25	
CH4+	9.0E-16		1.8E-15		1.5E-15		4.0E-23	
NH4+	4.7E-11		1.6E-11		3.5E-11		9.6E-26	
CH5+	4.0E-10		2.0E-10		1.1E-10		7.2E-20	
C2H2+	6.5E-11		1.8E-11		7.7E-12		1.3E-30	
C2H3+	1.3E-10		1.6E-10		4.6E-11		2.5E-31	
C2H4+	2.6E-10		1.1E-10		5.9E-11		4.0E-31	
C3H3+	2.4E-10		1.2E-10		5.3E-11		1.3E-35	
C3H2N+	6.8E-10		1.3E-10		1.0E-11		1.3E-33	
CH4N+	2.5E-12		1.3E-13		5.9E-14		4.3E-38	
CH6N+	2.5E-12		1.1E-13		4.7E-14		2.8E-38	
GRAIN0	1.3E-14		1.6E-14		2.5E-14		6.1E-14	
GRAIN-	2.6E-12		2.6E-12		2.6E-12		2.6E-12	

The differences between Models N(2100K) and Model D of HHL as regards surface species are caused principally by reactions of type (4) and (5), since the low activation energy coupled with the high surface abundance of H_2 at all times in this model ruins the production of complex molecules on grain surfaces. The carbon clusters and organo-nitrogen radicals are hydrogenated and cannot associate with each other, as in the early stages of Model D. Since the gas-phase chemistry is quite efficient in producing hydrogen-poor complex molecules, however, subsequent accretion on to the grains does result in considerable organic chemical surface concentrations, especially for the end products of reactions (4) and (5) and similar processes involving other radicals. In Table 3, the Model N(2100K)/Model D abundance ratios for surface species are shown for an 'early' time of 3.2×10^5 yr as well as for 1.0×10^7 yr. It can be seen that most surface organic molecule abundances decrease at most by an order of magnitude in the new model at 'early' time, whereas some molecules actually increase in abundance. Exceptions are radicals of the C_n and C_nH variety, which are hydrogenated rapidly to C_nH_2, and possess very small abundances in model N(2100K). The agreement between the surface results of Model D of HHL at times of 10^5–10^6 yr and quiescent cloud mantle observations is maintained (see Section 6).

The destructive power of H_2 concerning complex molecule production on grain surfaces can be mitigated somewhat if its sticking probability is significantly less than unity. In our model calculations, it has been assumed that the sticking probability for all neutral species on to grain surfaces is unity, whereas the sticking probability for positive atomic and molecular ions is zero. In all likelihood, the sticking coefficients for the light species H and H_2 are less than unity. d'Hendecourt et al. (1985) stated that the sticking

Table 3. Comparison of grain-surface molecular abundances between model N(2100K) and HHL model D.

	Model N(2100K)/Model D Abundance Ratio	
Surface species	t = 3.2 x 10^5 yr	t = 1.0 x 10^7 yr
CO	0.74	0.36
H_2O	1.10	1.05
CO_2	0.91	0.91
CH_4	1.00	1.00
C_2H_2	0.84	0.16
C_3	7.4 (-5)	1.2 (-6)
C_3H	1.7 (-4)	1.3 (-6)
C_3H_2	1.56	2.40
C_4H_2	0.69	0.48
C_5H_4	1.47	2.40
C_9H_2	1.73	3.33
CH_3OH	0.90	0.94
HC_3N	0.08	0.01
HC_5N	0.20	0.02
H_3C_5N	0.19	0.14
HC_9N	0.15	0.11
H_3C_9N	0.15	0.14

coefficient for H_2 on to 0.1-μm radius cold grains is not close to unity. Watson (1975) tabulated sticking coefficients for H_2 on to CO_2 and H_2O at 78 K of ≈ 0.5.

In our models, the surface abundance of H_2 is mainly determined by accretion and thermal evaporation rates. Lowering the sticking probability lowers the surface abundance of H_2 in a roughly linear manner. A lowered surface abundance of H_2 reduces the rate of hydrogenation reactions and promotes association between heavy species. However, we find that a sticking probability for H_2 of ≤ 0.001 is necessary to change dramatically the negative results of model N(2100K) as regards complex molecule formation on surfaces. Such a low sticking coefficient seems unphysical for 10-K grains.

Another possibility is that we have overestimated the influence of tunnelling reactions involving H_2 on grain surfaces. Given the relatively small rate coefficients utilized (Table 1), this seems unlikely. However, more accurate calculations of tunnelling probabilities can be obtained in the future for selected reactions once quantum chemical calculations of the potential energy surfaces become available (Herbst et al. 1991).

4 RATES FOR COSMIC RAY INDUCED DESORPTION

Following Léger et al. (1985), we assume that relativistic Fe nuclei with energies 20–70 MeV nucleon^{-1} deposit 0.4 MeV on the average into dust particles of radius 0.1 μm, impulsively heating them. With the standard expression for evaporative rates discussed below, a peak temperature of ≈ 70 K can be achieved rapidly compared with cooling via thermal evaporation and radiation. The rate coefficient for cosmic ray induced desorption $k_{crd}(i)$ for surface species i in units of s^{-1} is given by the expression

$$k_{crd}(i) = \frac{\int_{70\ K}^{10\ K} k_{evap}(i, T_d)[dt/dT_d]\, dT_d}{\int_{70\ K}^{10\ K} [dt/dT_d]\, dT_d} \qquad (13)$$

where the cooling of the grains as a function of time t is described by the function $T_d(t)$ and $k_{evap}(i)$, the thermal evaporation rate, is given by the standard expression (Tielens & Hagen 1982; Tielens & Allamandola 1987; Watson 1976; HHL)

$$k_{evap}(i) = \nu_0(i) \exp[-E_D(i)/T_d]. \qquad (14)$$

In expression (14), $\nu_0(i)$ is the characteristic adsorbate vibrational frequency for species i of $10^{12\text{-}13}$ s^{-1}, which can be calculated via a harmonic oscillator relation given in HHL, and $E_D(i)$ (K) is the adsorption (binding) energy of species i to the dust particle.

If there are sufficient volatile species on the grain surface, the cooling is initially dominated by thermal evaporation itself (Léger et al. 1985). For volatile species such as CO ($E_D(i) \approx 1200$ K), the half-life against desorption at 70 K is $\approx 10^{-5}$ s. By the time the temperature reaches 60 K, roughly 10^6 of these species per grain have been desorbed. For our model results in which cosmic ray induced desorption is not taken into account, the number of volatile species per grain often exceeds this amount.

To render equation (13) tractable for easy inclusion into our model calculations, we assume that much of the desorption occurs near 70 K. The temperature cycling of grains can then simply be regarded as consisting of periods at or near 70 K and periods well below this temperature, when desorption is minimal. Changing the variable of integration in equation (13) to time t, it is then easily shown that

$$k_{crd}(i) \approx f(70\ K)\, k_{evap}(i, 70\ K) \qquad (15)$$

where $f(70\ K)$, the fraction of the time spent by grains in the vicinity of 70 K, can be loosely defined as the ratio of the time-scale for cooling via desorption of volatiles ($\approx 10^{-5}$ s) to the time interval between successive heatings to 70 K. This latter number can be estimated to be 3.16×10^{13} s from the Fe cosmic ray flux in Léger et al. (1985) and a geometrical cross-section for grains of 0.1-μm radius. Then $f(70\ K) = 3.16 \times 10^{-19}$ is the 'duty cycle' of the grains at the elevated temperature. The cosmic ray induced desorption rates determined in this manner pertain only to dust particles with a significant mantle of volatile absorbates. They are insensitive to assumed peak grain temperatures because the f factor in equation (15) is inversely proportional to k_{evap} of the volatile material. For particles on which non-volatile species such as water ice are the only major components, our results are inaccurate, but because desorption of these species is so slow anyway, the discrepancy is unimportant.

The necessary adsorption energies $E_D(i)$ have been taken from previous sources (Tielens & Allamandola 1987; Allen & Robinson 1977), or calculated via the approach of Allen & Robinson (1977). These are listed in Table 4 along with the adopted cosmic ray induced desorption rates.

For non-reactive heavy species, the steady-state gas-phase abundance to surface abundance ratio is equal to the ratio $k_{crd}(i)/k_{acc}(i)$ of cosmic ray induced desorption to accretion rate coefficients. Illustrative desorption and accretion rate coefficients, the latter calculated according to the formula in HHL, are listed in Table 5 along with the ratios between them. For CO, for example, we find that, *in the absence of competitive chemical reactions*, cosmic ray desorption can maintain a ratio $n(CO)/n_s(CO)$ of 0.14, whereas for water, a less volatile material, the analogous ratio $n(H_2O)/n_s(H_2O)$ is 1.6×10^{-5}. The result for CO is similar to that derived in more detail by Léger et al. (1985), who obtained a ratio $n(CO)/n_s(CO) = 0.25$ for a cloud of density $n = 10^4$ cm^{-3}, half of our chosen gas density, despite the fact that these authors, utilizing a different expression for evaporative rates, obtained peak grain temperatures following cosmic ray heating of 25 K. Since the estimated adsorption energy E_D of ammonia is 1110 K, whereas that of methane is 1360 K, cosmic ray desorption processes will tend to maintain a large gas-phase abundance for the former. It should be remembered, however, that the adsorption energies we adopt are uncertain. For most of the larger molecules, the values of $E_D(i)$ are sufficiently large that cosmic ray induced desorption rates are too small to be of any significance.

5 RESULTS IN THE PRESENCE OF COSMIC RAY INDUCED DESORPTION

Two model calculations have been run. These are designated N(2100K, CR) and A(2100K, CR), where the designations are as discussed in Section 3 with the additional 'CR'

Table 4. Cosmic ray desorption rates, k_{crd}, and adsorption energies, E_D.

Species	k_{crd} (s^{-1})	E_D (K)	Species	k_{crd} (s^{-1})	E_D (K)
H	6.00E-09	3.50E+02	SIH4	6.50E-30	3.69E+03
H2	1.20E-09	4.50E+02	C2H3	4.60E-18	1.76E+03
HE	5.70E-08	1.00E+02	CHNH2	1.50E-16	1.51E+03
C	4.20E-12	8.00E+02	CH2NH	7.30E-17	1.56E+03
N	3.90E-12	8.00E+02	CH3N	2.20E-18	1.81E+03
O	3.70E-12	8.00E+02	C3H2	2.90E-20	2.11E+03
NA	6.70E-80	1.18E+04	CH2CN	1.80E-22	2.47E+03
MG	9.30E-40	5.30E+03	CH2CO	8.60E-23	2.52E+03
SI	8.30E-24	2.70E+03	HCOOH	4.00E-23	2.57E+03
S	4.20E-14	1.10E+03	CH2OH	1.40E-20	2.17E+03
FE	3.60E-33	4.20E+03	NH2OH	2.90E-24	2.77E+03
CH	3.00E-11	6.54E+02	C4H	9.60E-24	2.67E+03
NH	5.40E-11	6.04E+02	HC3N	1.40E-25	2.97E+03
OH	6.30E-15	1.26E+03	HC3O	4.60E-24	2.72E+03
C2	1.10E-14	1.21E+03	C5	3.70E-27	3.22E+03
NAH	3.80E-81	1.20E+04	C4N	3.60E-27	3.22E+03
MGH	2.60E-41	5.55E+03	C4S	6.10E-29	3.50E+03
FEH	1.00E-34	4.45E+03	C2H4	1.40E-19	2.01E+03
CN	1.60E-16	1.51E+03	CH2NH2	2.20E-18	1.81E+03
N2	9.80E-15	1.21E+03	CH3NH	4.40E-18	1.76E+03
CO	9.80E-15	1.21E+03	CH3OH	6.30E-20	2.06E+03
SIH	2.80E-25	2.94E+03	C3H3	6.10E-21	2.22E+03
NO	9.40E-15	1.21E+03	CH3CN	1.00E-23	2.27E+03
O2	9.10E-15	1.21E+03	H2C3N	6.70E-26	3.02E+03
HS	1.60E-16	1.50E+03	H2C3O	1.30E-25	2.97E+03
SIC	8.60E-29	3.50E+03	C4H2	2.80E-25	2.92E+03
SIO	8.20E-29	3.50E+03	C5H	1.10E-28	3.47E+03
CS	1.30E-19	2.00E+03	C6	1.20E-29	3.62E+03
NS	1.20E-19	2.00E+03	C5N	1.40E-31	3.93E+03
SO	1.20E-19	2.00E+03	CH3NH2	1.30E-19	2.01E+03
SIS	1.00E-30	3.80E+03	C2H5	3.30E-20	2.11E+03
S2	1.00E-19	2.00E+03	C3H4	1.80E-22	2.47E+03
CH2	4.60E-13	9.56E+02	C4H3	1.40E-25	2.97E+03
NH2	1.70E-12	8.56E+02	CH3CHO	6.00E-25	2.87E+03
H2O	1.40E-18	1.86E+03	H3C3N	1.90E-27	3.27E+03
SIH2	8.00E-27	3.19E+03	C5H2	2.70E-30	3.73E+03
MGH2	7.40E-43	5.80E+03	C6H	2.90E-31	3.88E+03
C2H	3.20E-16	1.46E+03	HC5N	4.10E-33	4.18E+03
N2H	1.50E-16	1.51E+03	C7	1.10E-34	4.43E+03
O2H	1.40E-16	1.51E+03	H4C3N	1.10E-28	3.47E+03
HS2	1.50E-21	2.30E+03	CH3C3N	3.10E-31	3.88E+03
HCN	4.60E-18	1.76E+03	H2C5N	2.00E-33	4.23E+03
HNC	1.50E-16	1.51E+03	C2H6	1.70E-21	2.32E+03
HCO	1.50E-16	1.51E+03	C4H4	4.00E-27	3.22E+03
HOC	4.50E-18	1.76E+03	C5H3	3.20E-31	3.88E+03
HCS	1.20E-19	2.00E+03	C6H2	8.50E-33	4.13E+03
HNO	1.40E-16	1.51E+03	C7H	3.30E-36	4.68E+03
H2S	2.40E-18	1.80E+03	C8	3.70E-37	4.83E+03
C3	1.20E-19	2.01E+03	C7N	5.10E-39	5.13E+03
O3	8.00E-23	2.52E+03	CH3OCH3	1.20E-24	2.82E+03
C2N	1.20E-19	2.01E+03	C2H5OH	1.20E-28	3.47E+03
C2O	1.10E-19	2.01E+03	CH3C4H	6.40E-31	3.83E+03
C2S	9.80E-23	2.50E+03	C5H4	3.80E-32	4.03E+03
NAOH	1.90E-87	1.30E+04	C6H3	1.00E-33	4.28E+03
OCN	1.10E-19	2.01E+03	C7H2	9.40E-38	4.93E+03
CO2	1.10E-22	2.50E+03	C8H	1.00E-38	5.08E+03
OCS	8.20E-26	3.00E+03	HC7N	1.30E-40	5.39E+03
SO2	3.00E-26	3.07E+03	C9	3.50E-42	5.64E+03
CH3	2.70E-14	1.16E+03	H3C5N	5.80E-35	4.48E+03
NH3	5.00E-14	1.11E+03	H5C3N	1.30E-29	3.62E+03
SIH3	2.30E-28	3.44E+03	CH3C5N	1.10E-38	5.08E+03
C2H2	3.90E-17	1.61E+03	H2C7N	6.20E-41	5.44E+03
N2H2	9.40E-15	1.21E+03	C6H4	1.20E-34	4.43E+03
H2O2	9.50E-23	2.52E+03	C7H3	1.10E-38	5.08E+03
H2S2	2.20E-23	2.60E+03	C8H2	2.60E-40	5.34E+03
CH2N	3.70E-17	1.61E+03	C9H	1.00E-43	5.89E+03
CHNH	4.90E-15	1.26E+03	C9N	1.60E-46	6.34E+03
H2CO	4.40E-18	1.76E+03	CH3C6H	2.20E-38	5.03E+03
CHOH	5.40E-19	1.91E+03	C7H4	1.10E-39	5.24E+03
HCCN	3.00E-21	2.27E+03	C8H3	3.10E-41	5.49E+03
HC2O	1.10E-19	2.01E+03	C9H2	2.90E-45	6.14E+03
HNCO	2.90E-21	2.27E+03	HC9N	4.50E-48	6.59E+03
C3H	3.10E-21	2.27E+03	H3C7N	1.80E-42	5.69E+03
H2CS	3.70E-21	2.25E+03	CH3C7N	3.40E-46	6.29E+03
C4	3.30E-22	2.42E+03	H2C9N	2.20E-48	6.64E+03
C3N	4.70E-24	2.72E+03	C8H4	3.70E-42	5.64E+03
C3O	7.70E-23	2.52E+03	C9H3	3.40E-46	6.29E+03
C3S	7.70E-26	3.00E+03	C9H4	4.00E-47	6.44E+03
CH4	1.60E-15	1.36E+03	H3C9N	5.50E-50	6.90E+03

referring to the presence of cosmic ray induced desorption. Of course, models with desorption differ most profoundly from those without non-thermal desorption at later times ($\geq 10^7$ yr), when the latter tend to lose most of the heavy gas-phase species. In the absence of chemical reactions, the ratio

Table 5. Some illustrative desorption and accretion rates (s^{-1}) at $T_{gas} = 10$ K and $n = 2 \times 10^4$ cm^{-3}.

Species	Cosmic ray-induced desorption rate k_{crd}	Accretion rate k_{acc}	k_{crd}/k_{acc}
H	6.0 (-9)	3.8 (-13)	1.6 (+4)
H_2	1.2 (-9)	2.7 (-13)	4.4 (+3)
C	4.2 (-12)	1.1 (-13)	3.8 (+1)
N_2	9.8 (-15)	7.2 (-14)	1.4 (-1)
CO	9.8 (-15)	7.2 (-14)	1.4 (-1)
CO_2	1.1 (-22)	5.8 (-14)	1.9 (-9)
H_2O	1.4 (-18)	9.0 (-14)	1.6 (-5)
NH_3	5.0 (-14)	9.3 (-14)	5.4 (-1)
CH_4	1.6 (-15)	9.5 (-14)	1.7 (-2)
H_2CO	4.4 (-18)	7.0 (-14)	6.3 (-5)
CH_3OH	6.3 (-20)	6.8 (-14)	9.3 (-7)
CH_3NH_2	1.3 (-19)	6.8 (-14)	1.9 (-6)
CH_3CH_2CN	1.3 (-29)	5.2 (-14)	2.5 (-16)

of gaseous to surface abundances of molecular species is given at steady state by the ratio of the desorption and accretion rates (Table 5). However, both ion–molecule chemistry and surface chemistry can be active for exceedingly long periods of time. Desorption puts species into the gas, ion–molecule chemistry processes all of them, and the neutral products eventually stick to grain surfaces (time-scale $\approx 10^6$ yr) where they undergo surface reactions. The cycle can be repeated many times for easily desorbed species and the results at exceedingly late stages are often not intuitive. Detailed results are presented for times until 10^8 yr, but we have run calculations until 10^9 yr. We find that the ratios of gaseous to surface abundances listed in Table 5 can be unreliable even for 'stable' molecules.

Before discussing our detailed results for models with non-thermal desorption, a broad overview of the dominant surface species might be helpful. The most abundant surface species at times of 3.2×10^5 and 1×10^7 yr for the models N(2100K), N(2100K, CR) and A(2100K, CR), which might be expected to differ most from the previous HHL results, are listed in Table 6 in the form of percentages of the total number of surface molecules. It can be seen that, as in HHL, water ice dominates both at early and late times, that methanol is also abundant at all times and conditions, and that the abundances of other species can be strongly affected by time and/or model conditions. Water ice is sufficiently abundant to build up 10–100 layers surrounding the initial grain cores.

5.1 Normal initial abundances

The results of model N(2100K, CR) are listed in Table 7 for times from 1×10^5–1×10^8 yr. At times before 10^6 yr, the differences between the results of this model and that of model N(2100K) (Table 2) are minimal. Thus the presence of reactions on the grain surface followed by desorption into the gas does not affect the gas-phase abundances at these times for the normal initial abundances. However, by 10^6 yr

Table 6. Grain surface composition – dominant species by per cent.

Model	N(2100K)		N(2100K,CR)			A(2100K,CR)		
t (yr)	3 x 10^5	1 x 10^7	3 x 10^5	1 x 10^7	1 x 10^8	3 x 10^5	1 x 10^7	1 x 10^8
				Fraction in percent by molecular number				
Species								
H_2	2.0	1.1	2.0	1.1	1.1	1.4	0.9	1.0
N_2	1.5	1 (-5)	1.4	0.3	0.3	5 (-6)	0.4	0.002
CO	4.3	5 (-12)	4.2	1 (-4)	9 (-5)	2 (-4)	2 (-4)	7 (-6)
H_2O	55	55	55	55	55	61	61	64
HCN	2.9	1.6	2.9	1.6	1.7	0.04	0.3	0.5
CO_2	10	5.8	10	5.8	5.8	0.002	0.006	0.008
NH_3	0.006	0.01	0.004	0.8	0.8	7.7	1.1	0.09
N_2H_2	1.9	4.0	1.8	2.7	2.7	0.03	3.0	0.2
H_2CO	3.4	12	3.4	12	11	5.8	10	11
HNCO	3.5	2.0	3.5	2.0	2.0	2 (-4)	0.02	0.04
CH_4	0.9	1.0	0.9	1.1	1.0	18	12	3.3
CH_3OH	13	17	13	17	17	5.8	10	11
CH_3NH_2	0.08	0.05	0.08	0.05	0.2	0.001	0.3	9.1
C_2H_6	0.3	0.3	0.3	0.3	0.3	0.04	0.1	0.2

Table 7. Gas and surface abundances for Model N(2100K, CR) expressed as a function of total $n(H_2) + 0.5\,n(H)$.

t(yr)	1.0 x 10^5		3.2 x 10^5		1.0 x 10^6		1.0 x 10^7		1.0 x 10^8	
Species	Gas	Surface	Gas	Surface	Gas	Surface	Gas	Surface	Gas	Surface
H	2.0E-04	3.8E-23	1.2E-04	6.5E-24	1.0E-04	2.7E-24	1.3E-04	3.3E-24	1.3E-04	3.3E-24
HE	2.8E-01	1.5E-21	2.8E-01	1.5E-21	2.8E-01	1.5E-21	2.8E-01	1.5E-21	2.8E-01	1.5E-21
C	3.7E-05	2.8E-14	1.8E-06	1.1E-18	8.4E-08	8.6E-23	6.6E-10	8.5E-19	6.1E-10	1.8E-18
N	3.1E-05	1.8E-13	1.5E-05	6.6E-14	1.7E-06	9.9E-16	3.4E-07	7.1E-16	3.3E-07	1.0E-15
O	1.9E-04	2.7E-13	7.6E-05	4.2E-17	6.2E-06	6.4E-21	7.5E-10	4.7E-23	7.4E-10	5.0E-23
NA	9.5E-10	1.0E-16	8.7E-10	5.5E-16	5.1E-10	7.7E-16	2.5E-12	3.1E-18	1.6E-42	2.0E-48
MG	3.9E-09	4.0E-16	3.3E-09	2.0E-15	1.9E-09	2.8E-15	4.7E-12	5.8E-18	9.3E-45	1.1E-50
SI	1.2E-08	1.2E-15	7.5E-09	4.3E-15	1.4E-09	1.9E-15	2.4E-18	2.7E-24	4.1E-25	4.5E-31
S	7.8E-08	1.4E-15	6.4E-08	5.5E-13	2.0E-08	2.0E-13	3.0E-12	1.3E-13	1.4E-12	8.6E-14
FE	1.1E-09	7.2E-17	8.5E-10	3.4E-16	4.3E-10	4.1E-16	1.5E-10	1.2E-16	2.3E-15	1.8E-21
H2	1.0E+00	4.0E-06	1.0E+00	4.0E-06	1.0E+00	4.0E-06	1.0E+00	4.0E-06	1.0E+00	4.0E-06
CH	4.2E-09	2.4E-18	9.5E-10	7.0E-24	1.2E-09	1.6E-26	3.5E-11	2.2E-26	3.1E-11	2.9E-26
NH	4.9E-10	5.3E-17	1.8E-10	2.9E-18	3.9E-10	6.7E-17	1.7E-08	2.5E-18	1.7E-08	3.8E-18
OH	2.1E-08	1.8E-16	3.5E-08	1.0E-16	1.1E-07	9.1E-18	1.6E-09	2.9E-20	1.5E-09	3.0E-21
C2	2.5E-08	3.4E-19	1.0E-08	1.7E-20	2.1E-08	3.5E-20	2.8E-12	4.6E-24	2.3E-12	3.8E-24
NAH	2.3E-13	1.6E-10	1.3E-13	6.8E-10	5.1E-14	1.8E-09	1.7E-16	4.0E-09	1.1E-46	4.0E-09
MGH	8.3E-13	4.0E-16	1.8E-13	2.0E-15	2.3E-14	2.8E-15	1.2E-19	5.8E-18	2.2E-80	1.1E-50
FEH	1.2E-32	1.1E-10	1.8E-31	4.6E-10	1.2E-30	1.1E-09	7.4E-30	3.9E-09	1.2E-29	6.0E-09
CN	7.2E-08	1.7E-17	2.2E-08	3.2E-20	9.6E-09	1.4E-20	2.9E-10	7.1E-22	2.7E-10	7.2E-22
N2	3.7E-08	4.5E-07	2.5E-07	2.9E-06	1.1E-06	3.8E-06	9.4E-07	1.1E-06	9.1E-07	1.0E-06
CO	6.7E-05	2.5E-06	6.0E-05	8.6E-06	1.4E-05	7.4E-06	1.1E-09	4.8E-10	1.0E-09	3.4E-10
SIH	2.8E-11	1.2E-15	1.2E-10	4.3E-15	2.5E-10	2.3E-15	9.0E-19	3.7E-24	1.5E-25	6.2E-31
NO	6.4E-09	3.2E-12	2.7E-08	6.6E-12	3.1E-08	2.5E-13	4.3E-11	6.6E-14	3.7E-11	5.3E-14
O2	1.2E-06	2.3E-12	5.0E-06	9.8E-09	4.1E-06	5.8E-06	1.0E-11	1.6E-12	8.0E-12	1.6E-14
HS	2.3E-11	5.8E-16	5.5E-11	5.8E-14	3.0E-11	5.5E-13	4.6E-14	6.9E-13	2.3E-14	3.2E-13
SIC	2.8E-11	2.5E-11	9.5E-12	3.3E-11	5.1E-12	4.2E-11	7.5E-22	4.5E-11	4.6E-28	4.5E-11
SIO	5.2E-10	1.5E-10	2.7E-10	3.0E-10	2.4E-11	4.3E-10	1.1E-21	4.4E-10	2.3E-27	4.4E-10
CS	6.8E-09	3.3E-16	3.2E-09	2.9E-13	5.6E-10	1.4E-10	1.9E-15	6.3E-11	9.3E-16	6.9E-11
NS	1.3E-10	8.5E-16	7.0E-11	6.1E-13	3.1E-12	5.0E-12	1.9E-15	9.7E-13	9.1E-16	5.1E-13
SO	1.1E-09	1.8E-15	8.9E-10	6.6E-13	1.2E-10	6.7E-11	9.2E-17	4.0E-17	4.4E-17	9.8E-18
SIS	1.2E-11	2.0E-12	6.3E-12	5.3E-12	7.6E-14	6.8E-12	1.1E-26	6.8E-12	7.1E-31	6.8E-12
S2	7.5E-17	4.0E-18	1.3E-15	1.8E-16	1.3E-15	2.4E-15	5.0E-22	2.9E-15	4.6E-22	2.9E-15
CH2	3.0E-07	4.6E-16	4.8E-08	1.8E-17	6.2E-09	6.0E-20	2.4E-10	1.3E-21	2.2E-10	1.7E-21
NH2	7.7E-09	7.6E-17	3.0E-09	1.9E-16	1.4E-08	1.8E-14	7.5E-07	9.1E-13	7.8E-07	8.7E-13
H2O	1.0E-06	5.0E-05	3.5E-07	1.1E-04	1.7E-07	1.7E-04	2.1E-09	2.0E-04	2.1E-09	2.0E-04
SIH2	1.3E-29	1.2E-15	1.3E-28	4.3E-15	3.4E-28	2.3E-15	1.1E-35	3.7E-24	7.1E-44	6.2E-31
MGH2	5.6E-40	6.5E-10	7.3E-39	2.7E-09	4.4E-38	6.8E-09	1.4E-37	1.4E-08	1.4E-37	1.4E-08
C2H	6.2E-08	4.6E-19	8.4E-09	3.2E-20	3.3E-09	4.2E-20	1.7E-12	7.6E-24	1.4E-12	6.3E-24
N2H	9.1E-15	4.2E-11	8.5E-14	1.4E-10	4.7E-13	3.3E-10	8.0E-13	3.8E-10	7.8E-13	3.7E-10
O2H	4.6E-20	9.6E-17	7.7E-20	9.5E-16	3.9E-15	4.3E-12	6.5E-18	2.1E-15	2.7E-23	1.3E-20
HS2	9.0E-14	6.4E-15	3.1E-13	7.2E-14	1.3E-13	3.6E-13	2.3E-20	4.1E-13	7.2E-21	4.1E-13
HCN	8.3E-08	4.2E-06	5.6E-09	5.9E-06	2.8E-09	5.9E-06	1.8E-10	5.9E-06	1.7E-10	6.0E-06

Table 7 – *continued*

t(yr)	1.0 x 10^5		3.2 x 10^5		1.0 x 10^6		1.0 x 10^7		1.0 x 10^8	
Species	Gas	Surface	Gas	Surface	Gas	Surface	Gas	Surface	Gas	Surface
HNC	4.1E-08	2.6E-07	3.2E-09	2.8E-07	2.8E-09	2.8E-07	1.4E-10	2.9E-07	1.3E-10	2.8E-07
HCO	2.2E-09	6.3E-13	6.8E-10	1.4E-11	4.8E-10	1.4E-11	1.6E-12	1.4E-12	1.5E-12	1.4E-12
HOC	2.7E-17	4.1E-12	2.5E-16	1.4E-11	8.4E-16	1.2E-11	5.8E-20	7.9E-16	3.6E-20	5.6E-16
HCS	6.3E-24	6.2E-18	5.3E-24	9.2E-19	5.0E-22	4.2E-16	2.2E-22	1.9E-16	4.5E-22	2.1E-16
HNO	2.4E-11	5.8E-13	2.7E-12	1.2E-09	3.2E-12	6.1E-08	4.1E-12	1.3E-07	2.9E-12	8.9E-08
H2S	5.0E-11	7.3E-11	9.3E-11	2.3E-09	7.2E-11	6.6E-08	1.6E-13	8.7E-08	7.6E-14	4.1E-08
C3	2.0E-08	3.7E-20	7.8E-09	1.4E-20	1.7E-08	3.2E-20	1.1E-13	2.0E-25	8.7E-14	1.6E-25
O3	7.7E-18	6.7E-08	6.9E-17	2.6E-07	1.5E-16	5.7E-08	9.9E-23	9.9E-17	1.4E-27	9.9E-19
C2N	2.5E-08	1.2E-15	5.7E-09	2.8E-15	1.5E-10	1.7E-16	3.0E-14	2.9E-20	2.6E-14	2.5E-20
C2O	1.2E-24	1.2E-18	9.5E-25	9.0E-23	2.6E-25	6.7E-26	9.2E-33	5.6E-32	8.5E-38	4.6E-32
C2S	9.8E-10	9.6E-17	3.7E-10	7.6E-13	1.8E-11	9.2E-11	6.4E-19	2.1E-21	2.7E-19	4.1E-22
NAOH	4.1E-14	6.4E-15	4.7E-15	1.2E-14	7.1E-16	1.5E-14	3.2E-20	1.6E-14	2.1E-50	1.6E-14
OCN	1.7E-09	1.3E-12	1.3E-09	1.7E-15	4.1E-10	4.6E-16	5.9E-17	1.7E-17	4.2E-17	2.8E-17
CO2	2.6E-07	8.6E-06	1.9E-07	2.1E-05	5.1E-09	2.1E-05	9.2E-15	2.1E-05	9.4E-15	2.1E-05
OCS	4.3E-08	4.7E-15	1.7E-08	8.0E-15	6.3E-10	8.5E-16	6.4E-18	7.5E-19	3.2E-18	8.6E-19
SO2	2.6E-10	2.8E-08	6.6E-11	7.0E-08	2.5E-12	7.1E-08	3.9E-20	7.1E-08	2.0E-20	7.1E-08
CH3	4.9E-09	3.3E-15	5.5E-09	3.0E-15	3.0E-08	1.4E-16	2.7E-08	4.8E-17	2.4E-08	6.2E-17
NH3	1.5E-08	6.5E-09	4.1E-09	9.0E-09	1.7E-08	2.0E-08	9.2E-07	2.8E-06	9.7E-07	2.9E-06
SIH3	3.9E-31	1.2E-15	3.9E-30	4.3E-15	1.0E-29	2.3E-15	3.8E-37	3.7E-24	2.1E-45	6.2E-31
C2H2	2.6E-07	7.0E-08	1.5E-07	6.9E-08	3.9E-08	8.3E-08	2.4E-11	3.6E-11	2.1E-11	3.0E-11
N2H2	1.4E-08	1.1E-06	1.1E-07	3.7E-06	1.8E-07	8.7E-06	1.2E-07	9.9E-06	1.2E-07	9.7E-06
H2O2	8.4E-20	3.4E-10	2.0E-19	2.5E-10	9.5E-16	2.0E-06	1.9E-16	9.3E-08	5.6E-23	3.8E-14
H2S2	4.0E-16	2.0E-17	7.2E-15	9.6E-16	8.1E-15	1.4E-14	6.3E-22	1.7E-14	3.5E-22	1.7E-14
CH2N	1.3E-19	1.9E-15	5.7E-19	1.6E-16	1.2E-19	2.0E-20	1.3E-25	2.4E-22	2.3E-25	4.4E-22
CHNH	8.0E-20	3.8E-19	5.0E-20	3.8E-25	1.1E-20	6.0E-26	1.4E-28	1.9E-27	2.5E-28	3.7E-27
H2CO	1.8E-07	3.2E-06	3.9E-08	6.9E-06	9.0E-09	3.2E-05	2.7E-11	4.2E-05	2.8E-11	4.1E-05
CHOH	3.3E-18	4.1E-12	3.0E-17	1.4E-11	1.0E-16	1.2E-11	7.1E-21	7.9E-16	4.4E-21	5.6E-16
HCCN	4.3E-24	1.2E-15	4.2E-23	2.8E-15	3.3E-23	1.7E-16	1.4E-27	2.9E-20	1.2E-27	2.5E-20
HC2O	1.2E-24	1.2E-18	9.5E-25	9.0E-23	2.6E-25	6.7E-26	1.2E-32	5.6E-32	8.6E-38	4.6E-32
HNCO	1.8E-14	4.0E-06	1.2E-13	7.2E-06	2.9E-13	7.2E-06	3.6E-13	7.2E-06	3.6E-13	7.2E-06
C3H	3.9E-08	1.1E-19	5.4E-09	2.5E-20	1.4E-09	3.5E-20	5.7E-15	2.1E-25	4.7E-15	1.7E-25
H2CS	9.2E-10	3.6E-10	3.1E-10	5.9E-10	1.1E-11	1.0E-09	8.8E-16	1.6E-09	4.5E-16	4.8E-08
C4	1.7E-08	3.2E-20	5.3E-09	1.0E-20	1.2E-08	2.2E-20	1.3E-15	2.5E-27	1.0E-15	1.9E-27
C3N	2.2E-08	2.4E-15	5.4E-09	2.3E-15	7.5E-10	7.7E-16	1.7E-14	1.5E-20	1.4E-14	1.2E-20
C3O	3.0E-11	3.2E-18	5.3E-11	2.2E-17	4.6E-12	4.6E-18	1.4E-19	1.2E-25	1.2E-19	1.0E-25
C3S	4.0E-10	2.6E-10	1.3E-10	5.3E-10	6.6E-12	5.9E-10	3.4E-21	6.9E-10	1.4E-21	6.9E-10
CH4	1.8E-06	6.2E-07	1.3E-06	1.9E-06	1.6E-07	2.6E-06	3.7E-08	3.8E-06	3.5E-08	3.6E-06
SIH4	2.8E-26	2.9E-09	2.2E-25	7.7E-09	9.5E-25	1.4E-08	1.5E-24	1.6E-08	1.5E-24	1.6E-08
C2H3	5.3E-08	4.4E-14	1.4E-08	7.4E-14	4.8E-09	8.7E-14	2.1E-12	3.7E-17	1.8E-12	3.1E-17
CHNH2	8.8E-22	3.3E-19	5.8E-22	1.4E-23	1.3E-22	7.3E-24	8.8E-25	4.2E-22	1.1E-24	5.1E-22
CH2NH	8.9E-10	3.2E-08	3.1E-11	3.8E-08	2.4E-11	3.8E-08	6.0E-11	3.8E-08	5.8E-11	4.3E-08
CH3N	4.2E-20	1.4E-14	4.3E-19	2.7E-14	1.1E-19	4.6E-17	2.9E-22	9.2E-18	5.1E-22	1.6E-17
C3H2	2.4E-08	6.1E-09	7.1E-09	9.0E-09	2.0E-09	1.5E-08	7.2E-15	2.2E-13	5.9E-15	1.1E-13
CH2CN	2.8E-08	3.5E-15	9.8E-10	3.2E-15	2.3E-11	2.0E-16	3.4E-14	6.2E-20	3.0E-14	5.3E-20
CH2CO	3.6E-08	5.8E-09	2.9E-09	1.1E-08	6.9E-11	1.2E-08	3.1E-17	1.2E-08	2.9E-17	1.2E-08
HCOOH	1.0E-09	8.5E-11	1.2E-09	5.2E-10	8.9E-11	1.0E-09	5.5E-17	1.1E-09	5.4E-17	1.1E-09
CH2OH	8.6E-20	4.1E-12	7.7E-19	1.4E-11	2.7E-18	1.2E-11	1.9E-22	7.9E-16	1.1E-22	5.6E-16
NH2OH	1.4E-24	2.4E-13	6.8E-24	4.7E-13	1.1E-22	6.1E-12	9.3E-21	2.1E-10	1.1E-20	2.4E-10
C4H	1.2E-07	2.6E-19	1.0E-08	3.0E-20	2.1E-09	2.6E-20	1.3E-16	2.8E-27	9.9E-17	2.2E-27
HC3N	5.8E-08	5.2E-09	5.5E-09	6.9E-09	4.9E-10	3.5E-09	1.2E-14	3.5E-14	9.8E-15	2.4E-14
HC3O	4.7E-29	3.2E-18	3.4E-28	2.2E-17	7.6E-28	4.6E-18	4.5E-34	1.2E-25	8.9E-36	1.0E-25
C5	8.7E-09	1.6E-20	1.5E-09	2.9E-21	2.0E-09	3.8E-21	2.7E-18	5.0E-30	2.0E-18	3.8E-30
C4N	2.9E-09	3.1E-10	4.1E-10	7.5E-10	1.5E-11	8.4E-10	2.9E-17	8.7E-10	2.1E-22	8.7E-10
C4S	1.6E-10	2.8E-11	1.1E-11	4.1E-11	8.4E-13	4.4E-11	1.9E-23	4.5E-11	7.4E-24	4.5E-11
C2H4	1.2E-09	2.4E-09	7.6E-10	4.0E-09	2.7E-11	4.8E-09	1.4E-13	2.1E-12	1.2E-13	1.7E-12
CH2NH2	1.4E-23	4.8E-19	1.1E-23	8.6E-20	3.5E-24	6.5E-20	1.8E-24	5.9E-20	2.3E-24	7.1E-20
CH3NH	1.0E-19	1.5E-14	9.0E-19	2.7E-14	2.7E-19	1.0E-15	1.2E-21	1.9E-17	2.2E-21	3.5E-17
CH3OH	2.7E-09	1.1E-05	9.7E-11	2.7E-05	8.7E-12	5.2E-05	5.4E-13	6.2E-05	5.6E-13	6.2E-05
C3H3	1.8E-10	3.6E-14	6.9E-11	8.0E-15	2.7E-12	1.3E-14	3.3E-16	2.0E-19	2.8E-16	1.1E-19
CH3CN	3.7E-09	6.8E-09	2.2E-11	1.5E-08	2.3E-12	1.7E-08	6.4E-15	1.7E-08	5.6E-15	1.7E-08
H2C3N	3.7E-28	4.4E-15	2.5E-27	5.8E-15	4.2E-27	3.0E-15	1.2E-31	3.0E-20	2.5E-32	2.0E-20
H2C3O	7.8E-24	3.0E-11	3.4E-23	4.7E-11	1.2E-22	6.9E-11	1.8E-22	7.2E-11	1.8E-22	7.2E-11
C4H2	2.0E-08	1.0E-08	3.5E-09	1.1E-08	2.2E-10	1.1E-08	2.8E-16	7.3E-14	2.2E-16	1.3E-15
C5H	4.2E-09	2.5E-20	1.8E-10	3.2E-21	1.5E-11	3.9E-21	4.5E-20	5.2E-30	3.4E-20	3.9E-30
C6	3.4E-09	6.2E-21	3.6E-10	6.6E-22	2.6E-10	4.8E-22	7.3E-21	1.4E-32	5.2E-21	9.6E-33
C5N	2.9E-09	1.7E-16	3.8E-10	1.3E-16	1.6E-11	1.4E-17	3.4E-19	2.4E-25	2.6E-19	1.8E-25
CH3NH2	6.5E-10	9.2E-08	2.2E-11	1.5E-07	1.6E-11	1.6E-07	3.8E-11	2.0E-07	3.7E-11	6.5E-07
C2H5	4.3E-21	4.4E-14	1.2E-20	7.2E-14	3.4E-20	8.6E-14	1.8E-23	3.8E-17	1.5E-23	3.2E-17
C3H4	2.3E-10	2.6E-07	2.5E-10	3.1E-07	6.5E-12	3.2E-07	8.4E-16	4.1E-07	7.1E-16	4.1E-07

Table 7 – *continued*

t(yr)	1.0 x 10^5		3.2 x 10^5		1.0 x 10^6		1.0 x 10^7		1.0 x 10^8	
Species	Gas	Surface	Gas	Surface	Gas	Surface	Gas	Surface	Gas	Surface
C4H3	1.9E-27	8.6E-15	9.2E-27	9.5E-15	1.8E-26	9.1E-15	1.8E-30	6.2E-20	3.0E-33	1.1E-21
CH3CHO	1.4E-11	4.7E-12	2.5E-12	2.9E-11	2.1E-13	8.2E-11	2.3E-18	1.2E-10	2.1E-18	2.0E-10
H3C3N	2.0E-10	2.6E-10	2.1E-11	3.6E-10	1.5E-13	1.9E-10	2.1E-17	1.8E-15	1.8E-17	1.2E-15
C5H2	4.3E-09	1.1E-09	4.2E-10	1.2E-09	1.7E-11	1.3E-09	1.6E-19	7.9E-15	1.3E-19	2.0E-18
C6H	2.0E-09	1.0E-20	6.7E-11	7.9E-22	4.6E-12	4.9E-22	9.8E-23	1.4E-32	7.0E-23	9.8E-33
HC5N	5.1E-09	3.7E-10	1.9E-10	4.2E-10	2.6E-12	1.7E-10	4.2E-20	2.8E-16	3.2E-20	2.5E-19
C7	1.5E-09	2.7E-21	1.2E-10	2.2E-22	6.8E-11	1.2E-22	3.4E-23	6.1E-35	2.3E-23	4.1E-35
H4C3N	6.0E-31	4.3E-15	4.1E-30	5.9E-15	7.2E-30	3.1E-15	2.2E-34	3.0E-20	4.2E-35	2.0E-20
CH3C3N	3.8E-10	4.7E-11	8.5E-12	7.8E-11	8.5E-14	7.9E-11	7.4E-20	7.9E-11	5.8E-20	7.9E-11
H2C5N	7.4E-37	3.0E-16	5.0E-36	3.4E-16	7.7E-36	1.4E-16	3.2E-40	2.3E-22	9.2E-45	2.0E-25
C2H6	1.8E-15	4.9E-07	6.2E-15	5.9E-07	1.4E-14	7.2E-07	2.5E-14	1.0E-06	2.5E-14	1.0E-06
C4H4	1.4E-22	2.4E-08	9.5E-22	4.4E-08	3.0E-21	5.7E-08	7.9E-21	1.0E-07	7.9E-21	1.0E-07
C5H3	4.9E-34	8.7E-16	2.3E-33	9.9E-16	4.8E-33	1.0E-15	7.6E-37	6.6E-21	1.1E-41	1.7E-24
C6H2	4.5E-09	5.5E-10	6.8E-10	6.1E-10	4.6E-11	3.7E-10	2.6E-21	2.1E-15	1.9E-21	6.1E-21
C7H	1.1E-09	4.7E-21	1.8E-11	2.6E-22	1.0E-12	1.3E-22	4.5E-25	6.2E-35	3.1E-25	4.2E-35
C8	7.8E-10	1.4E-21	4.1E-11	7.2E-23	2.3E-11	4.0E-23	3.6E-25	6.3E-37	2.3E-25	4.1E-37
C7N	5.4E-10	2.8E-17	2.6E-11	7.9E-18	8.1E-13	6.0E-19	1.6E-24	1.0E-30	1.1E-24	6.8E-31
CH3OCH3	2.6E-12	2.3E-13	1.5E-14	5.3E-13	1.5E-16	5.3E-13	3.8E-19	5.3E-13	3.7E-19	5.3E-13
C2H5OH	2.9E-12	1.1E-11	7.5E-13	7.6E-11	1.1E-14	1.3E-10	7.1E-19	1.4E-10	6.4E-19	1.4E-10
CH3C4H	3.3E-09	2.4E-10	3.8E-10	8.4E-10	8.4E-12	8.9E-10	1.4E-19	9.1E-10	1.1E-19	9.1E-10
C5H4	3.3E-28	4.2E-09	1.5E-27	6.3E-09	4.2E-27	7.7E-09	9.9E-27	1.2E-08	9.9E-27	1.2E-08
C6H3	7.2E-37	4.4E-16	3.6E-36	4.9E-16	6.4E-36	3.0E-16	9.8E-40	1.7E-21	1.1E-46	4.9E-27
C7H2	9.2E-10	2.0E-10	2.8E-11	1.5E-10	1.3E-12	7.8E-11	7.6E-25	5.0E-16	5.3E-25	1.9E-23
C8H	1.1E-09	3.3E-21	1.4E-11	9.7E-23	8.1E-13	4.1E-23	5.9E-27	6.4E-37	3.8E-27	4.2E-37
HC7N	1.1E-09	7.0E-11	2.2E-11	6.0E-11	5.3E-13	2.1E-11	1.2E-24	4.3E-17	8.2E-25	1.5E-24
C9	2.2E-10	3.7E-22	9.8E-12	1.7E-23	3.7E-12	6.2E-24	4.8E-28	8.2E-40	3.1E-28	5.2E-40
H3C5N	3.4E-32	5.1E-10	3.8E-31	1.3E-09	1.4E-30	1.6E-09	2.4E-30	1.8E-09	2.4E-30	1.8E-09
H5C3N	1.3E-25	7.9E-09	1.2E-24	2.0E-08	4.5E-24	2.6E-08	8.2E-24	3.3E-08	8.2E-24	3.3E-08
CH3C5N	2.6E-11	2.6E-12	1.2E-13	4.0E-12	3.5E-16	4.0E-12	2.3E-25	4.0E-12	1.6E-25	4.0E-12
H2C7N	4.3E-45	5.5E-17	2.5E-44	4.7E-17	3.5E-44	1.6E-17	3.6E-48	3.4E-23	1.9E-57	1.2E-30
C6H4	4.0E-31	1.8E-09	2.0E-30	2.8E-09	6.2E-30	3.4E-09	1.2E-29	4.4E-09	1.2E-29	4.4E-09
C7H3	3.0E-42	1.6E-16	1.2E-41	1.2E-16	1.7E-41	6.2E-17	4.0E-45	4.0E-22	4.1E-54	1.5E-29
C8H2	5.5E-10	1.4E-10	4.1E-11	9.7E-11	4.1E-13	4.1E-11	2.2E-26	2.8E-16	1.4E-26	1.9E-25
C9H	1.4E-10	6.0E-22	9.6E-13	1.8E-23	1.5E-14	6.3E-24	7.0E-30	8.4E-40	4.5E-30	5.3E-40
C9N	6.8E-11	3.2E-18	1.5E-12	4.1E-19	7.2E-15	4.8E-21	1.1E-29	5.8E-36	6.7E-30	3.6E-36
CH3C6H	9.5E-11	6.2E-12	3.5E-12	1.6E-11	2.7E-14	1.7E-11	1.8E-25	1.7E-11	1.3E-25	1.7E-11
C7H4	1.4E-36	6.6E-10	6.9E-36	9.9E-10	2.0E-35	1.1E-09	3.6E-35	1.3E-09	3.6E-35	1.3E-09
C8H3	5.7E-45	1.1E-16	2.2E-44	7.6E-17	3.0E-44	3.2E-17	9.0E-48	2.2E-22	1.2E-58	1.5E-31
C9H2	2.1E-10	2.8E-11	2.0E-12	1.8E-11	2.0E-14	7.2E-12	1.3E-29	3.3E-17	8.6E-30	2.3E-28
HC9N	1.3E-10	8.1E-12	1.3E-12	6.0E-12	4.8E-15	1.9E-12	8.2E-30	4.1E-18	5.2E-30	8.2E-30
H3C7N	2.0E-40	9.5E-11	2.1E-39	2.2E-10	7.7E-39	2.7E-10	1.4E-38	2.9E-10	1.4E-38	2.9E-10
CH3C7N	5.3E-12	4.8E-13	1.3E-14	7.2E-13	6.5E-17	7.2E-13	6.2E-30	7.2E-13	4.0E-30	7.2E-13
H2C9N	1.8E-53	6.3E-18	9.7E-53	4.6E-18	1.3E-52	1.5E-18	2.7E-56	3.2E-24	4.2E-70	6.4E-36
C8H4	1.8E-39	3.2E-10	1.2E-38	5.3E-10	3.7E-38	6.1E-10	6.9E-38	7.1E-10	6.9E-38	7.1E-10
C9H3	1.2E-50	2.2E-17	4.9E-50	1.4E-17	6.4E-50	5.6E-18	1.8E-53	2.6E-23	1.7E-66	1.8E-34
C9H4	4.0E-45	6.4E-11	2.6E-44	1.1E-10	8.2E-44	1.2E-10	1.5E-43	1.3E-10	1.5E-43	1.3E-10
H3C9N	7.3E-49	1.1E-11	7.5E-48	2.5E-11	2.7E-47	2.9E-11	5.0E-47	3.1E-11	5.0E-47	3.1E-11
E	3.6E-08		4.1E-08		5.0E-08		4.6E-08		4.4E-08	
H+	3.0E-10		8.4E-10		1.4E-09		6.8E-10		6.5E-10	
HE+	6.4E-10		8.3E-10		2.5E-09		3.8E-09		3.7E-09	
C+	2.9E-09		8.0E-09		7.9E-09		3.1E-12		2.7E-12	
N+	5.6E-12		2.9E-12		1.6E-11		1.8E-10		1.8E-10	
O+	2.3E-15		1.4E-14		2.3E-14		1.8E-16		1.7E-16	
NA+	2.9E-09		2.4E-09		1.7E-09		6.1E-12		3.8E-42	
MG+	9.5E-09		8.0E-09		5.3E-09		9.9E-12		1.9E-44	
SI+	1.4E-11		3.6E-11		9.0E-12		5.9E-20		1.0E-26	
S+	1.2E-10		4.9E-10		1.0E-10		1.4E-15		6.2E-16	
FE+	4.8E-09		4.7E-09		4.4E-09		1.9E-09		3.0E-14	
O2+	9.1E-12		1.0E-10		1.3E-10		1.7E-16		1.3E-16	
CH+	1.8E-13		1.6E-14		3.8E-15		2.0E-16		1.8E-16	
SO+	1.1E-11		2.0E-11		6.4E-12		1.2E-18		5.5E-19	
H3+	2.2E-09		4.0E-09		1.7E-08		3.0E-08		2.9E-08	
CH2+	2.7E-13		3.9E-14		1.7E-14		6.8E-16		6.1E-16	
NH2+	1.9E-14		7.8E-15		4.6E-14		1.4E-12		1.4E-12	
HCO+	5.2E-09		8.1E-09		6.6E-09		8.3E-13		8.3E-13	
HOC+	4.9E-10		5.8E-10		4.5E-10		5.3E-14		5.4E-14	
N2H+	9.8E-13		1.5E-11		2.0E-10		3.1E-10		3.1E-10	
C2N+	3.4E-10		6.1E-11		2.9E-11		7.3E-16		6.4E-16	
HCS+	2.0E-11		3.8E-11		2.5E-11		1.2E-16		6.1E-17	

Table 7 – *continued*

t(yr)	1.0 x 10^5		3.2 x 10^5		1.0 x 10^6		1.0 x 10^7		1.0 x 10^8	
Species	Gas	Surface	Gas	Surface	Gas	Surface	Gas	Surface	Gas	Surface
OCS+	2.0E-10		1.4E-10		5.9E-12		2.1E-21		1.1E-21	
H3O+	2.0E-09		1.3E-09		1.0E-09		1.4E-11		1.3E-11	
HCO2+	4.5E-12		6.7E-12		8.0E-13		2.8E-18		3.0E-18	
H2CN+	4.1E-10		5.7E-11		8.5E-11		5.8E-12		5.5E-12	
CH3+	3.4E-10		7.0E-11		3.1E-11		1.4E-12		1.3E-12	
NH3+	1.5E-12		7.3E-13		5.4E-12		2.9E-10		2.9E-10	
CH4+	9.0E-16		1.8E-15		1.4E-15		1.7E-15		1.5E-15	
NH4+	4.7E-11		1.9E-11		1.2E-10		8.4E-09		9.0E-09	
CH5+	4.0E-10		2.0E-10		1.2E-10		3.1E-11		2.9E-11	
C2H2+	6.5E-11		1.8E-11		8.5E-12		3.6E-15		3.0E-15	
C2H3+	1.3E-10		1.6E-10		4.9E-11		3.2E-14		2.8E-14	
C2H4+	2.6E-10		1.1E-10		6.8E-11		3.8E-14		3.3E-14	
C3H3+	2.4E-10		1.2E-10		5.9E-11		2.8E-16		2.3E-16	
C3H2N+	6.8E-10		1.3E-10		2.7E-11		9.6E-16		8.2E-16	
CH4N+	2.6E-12		1.5E-13		2.4E-13		8.1E-13		8.1E-13	
CH6N+	2.5E-12		1.3E-13		1.9E-13		6.0E-13		6.0E-13	
GRAIN0	1.3E-14		1.6E-14		2.4E-14		2.9E-14		2.9E-14	
GRAIN-	2.6E-12		2.6E-12		2.6E-12		2.6E-12		2.6E-12	

the picture begins to change, and cosmic ray induced desorption permits substantial abundances of heavy gas-phase molecules to persist, especially for (i) the smaller, more saturated molecules with relatively low values of E_D, and (ii) gaseous species formed from the desorbed molecules. Still, even for most of the smaller molecules, gas-phase abundances are lower at 10^{7-8} yr than at 10^{5-6} yr, as can be seen in Fig. 1. Ammonia is an exception (as is NH_2). After 10^6 yr, ammonia is formed in the gas via ion–molecule destruction of desorbed and fragile N_2H_2; it reaches high gas-phase abundances that far exceed observed values in quiescent clouds and are comparable to those in star-forming regions such as the Orion Hot Core (Blake et al. 1987). For all of the small gas-phase species depicted in Fig. 1, it can be seen that a quasi-steady state is reached at 10^7 yr and maintained until at least 10^8 yr.

The existence of desorption can enhance the overall (gaseous + surface) abundances of relatively unhydrogenated molecules compared with non-desorption models at late times. Grain hydrogenation is faster than desorption, but gas-phase processes reconvert some of the hydrogenated desorbed material back to the unhydrogenated state. An example occurs for N_2, where surface formation and desorption of N_2H_2 is followed by gas-phase processing back into gaseous N_2, which is subsequently followed by accretion. Another example occurs for CO, although at late stages this molecule is not particularly abundant in either phase.

As for complex molecules, gas-phase abundances are quite small for times later than 10^6 yr because of the slow rate of desorption; even these small values are too high for selected species, since we have not included gas-phase depletion reactions for many of the saturated species formed only on dust surfaces. The surface abundances of hydrogenated complex molecules (see HHL for a discussion of the extent of saturation permitted) reach large asymptotic abundances by $\approx 3 \times 10^5$ yr, while the less saturated complex molecules are gradually depleted via slow hydrogenation.

5.2 Atomic initial abundances

The results of model A(2100K, CR) are listed in Table 8. The presence of cosmic ray induced desorption introduces major changes at all times for this set of initial abundances. At early times, the rapid grain surface formation of simple ices (H_2O, NH_3, CH_4) occurs. Of these three species, ammonia, with the lowest adsorption energy, comes off the grains fastest, and the resulting gas-phase fractional abundance of ammonia at 3.2×10^5 yr exceeds 1×10^{-6} (with respect to H_2), which is 100–1000 times its value in models without desorption. The 'daughter' molecule NH_2, produced via gas-phase destruction of NH_3, also has a large fractional abundance in the gas phase at these times. The increases in gaseous abundances for water, methane and other 'ices', such as H_2S, are far more modest.

The large infusion of ammonia into the gas phase has serious implications for the gas-phase chemistry at 'early times', enhancing the abundance of other nitrogen-containing species in the gas, including organo–nitrogen molecules. The gaseous cyanopolyyne abundances at their peak still lie below those calculated for models with normal initial abundances. For example, the peak fractional abundances of gaseous HC_3N and HC_9N in model A(2100K, CR) are 1.4×10^{-8} and 1.5×10^{-12}, whereas they are greater in model N(2100K, CR) by factors of 4 and 100, respectively.

After 10^6 yr, adsorption tends to decrease gas-phase abundances despite the existence of non-thermal desorption, as can be seen in Fig. 2, where the fractional abundances of selected small gas-phase molecules calculated in model A(2100K, CR) are plotted against time. Abundances of most gaseous neutral species, in particular oxygen-containing molecules, decline rapidly to reach quasi-steady state values at about 10^7 yr. The most saturated forms of these species have large adsorption energies and desorb slowly. Gaseous abundances of easily desorbed, saturated species such as NH_3 and CH_4 decrease slowly, and maintain high

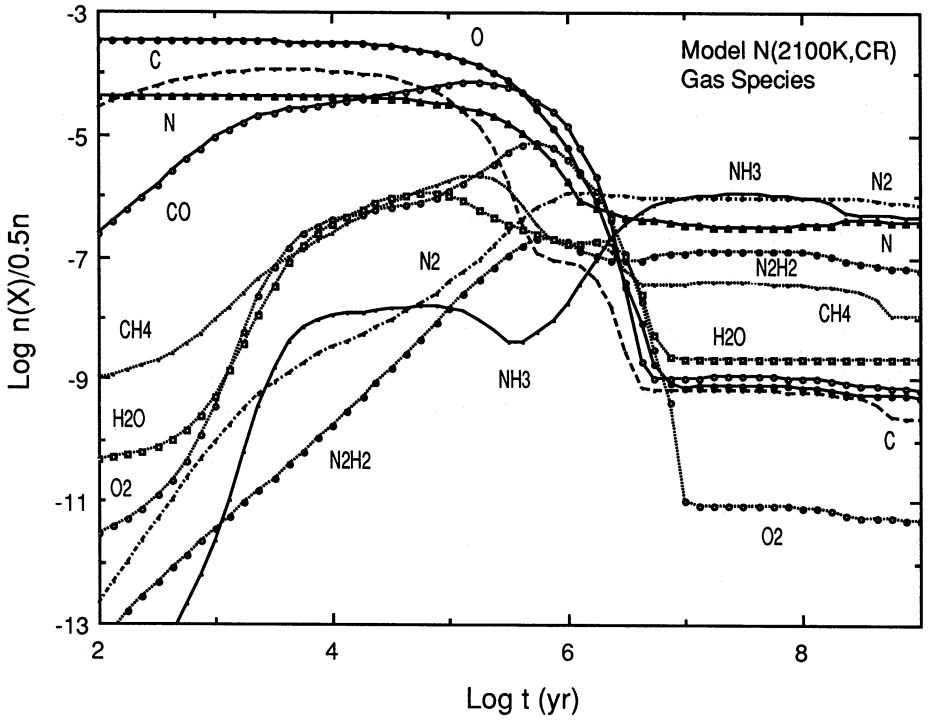

Figure 1. Fractional abundances (with respect to $n/2$) of selected small molecules in the gas phase are depicted as functions of time for model N(2100K, CR). Although cosmic ray induced desorption allows the persistence of sizeable abundances past 10^6 yr, these abundances are generally lower than at earlier times.

Table 8. Gas and surface abundances for Model A(2100K, CR) expressed as fractions of total $n(H_2)+0.5\,n(H)$.

t(yr)	1.0 x 10^5		3.2 x 10^5		1.0 x 10^6		1.0 x 10^7		1.0 x 10^8	
Species	Gas	Surface	Gas	Surface	Gas	Surface	Gas	Surface	Gas	Surface
H	6.0E-01	2.0E-17	4.4E-02	1.1E-19	1.3E-04	4.6E-24	1.2E-04	2.5E-24	1.2E-04	3.4E-23
HE	2.8E-01	1.5E-21	2.8E-01	1.5E-21	2.8E-01	1.5E-21	2.8E-01	1.5E-21	2.8E-01	1.5E-21
C	6.0E-05	1.8E-17	4.5E-06	1.6E-16	2.7E-07	5.3E-22	7.1E-09	8.0E-18	6.5E-10	4.6E-17
N	3.2E-05	8.5E-18	1.8E-05	8.2E-16	3.5E-06	2.5E-15	3.8E-07	4.9E-16	7.2E-08	4.9E-15
O	2.2E-04	5.4E-17	8.1E-05	4.0E-17	3.8E-06	7.9E-21	8.3E-10	9.8E-23	3.7E-10	2.3E-20
NA	4.5E-10	9.4E-23	9.8E-10	3.6E-20	7.7E-10	6.9E-16	6.1E-14	1.0E-19	1.7E-33	2.1E-40
MG	1.9E-09	3.9E-22	3.9E-09	1.4E-19	2.9E-09	2.5E-15	1.1E-13	1.8E-19	1.3E-35	1.5E-42
SI	1.3E-08	2.4E-21	8.1E-09	2.7E-19	1.5E-09	1.2E-15	2.2E-18	3.2E-24	2.9E-25	3.2E-32
S	1.3E-07	2.3E-20	5.6E-08	5.0E-18	1.8E-08	4.8E-13	4.1E-12	1.7E-13	8.1E-15	1.3E-19
FE	2.0E-10	2.7E-23	9.5E-10	2.2E-20	9.9E-10	5.7E-16	7.1E-11	7.4E-17	2.5E-14	1.9E-21
H2	7.0E-01	4.5E-06	9.8E-01	4.0E-06	1.0E+00	4.0E-06	1.0E+00	4.0E-06	1.0E+00	4.0E-06
CH	1.3E-08	9.1E-18	9.6E-10	2.2E-20	1.9E-09	5.2E-26	3.8E-10	4.6E-25	3.9E-10	5.7E-22
NH	2.2E-09	8.5E-18	2.1E-08	8.1E-16	4.1E-08	3.6E-17	2.2E-08	2.6E-18	5.9E-09	4.5E-17
OH	1.1E-08	4.5E-17	3.5E-08	1.1E-16	8.7E-08	6.4E-18	1.5E-09	3.6E-20	2.4E-09	3.6E-21
C2	4.9E-08	8.9E-21	1.3E-08	2.1E-20	3.6E-08	5.9E-20	2.4E-10	3.9E-22	1.1E-10	1.9E-22
NAH	3.5E-14	9.8E-11	1.8E-13	5.4E-10	1.1E-13	2.1E-09	4.4E-18	4.0E-09	9.4E-38	4.0E-09
MGH	1.6E-14	3.9E-22	4.1E-13	1.4E-19	9.6E-14	2.5E-15	8.1E-23	1.8E-19	1.3E-64	1.5E-42
FEH	6.3E-33	3.2E-11	7.5E-32	2.5E-10	1.2E-30	1.4E-09	1.0E-29	5.3E-09	1.2E-29	6.0E-09
CN	7.6E-08	1.3E-20	1.3E-07	2.0E-19	1.8E-07	2.6E-19	3.6E-09	9.0E-21	3.1E-10	6.0E-22
N2	1.9E-08	3.5E-15	3.5E-07	1.4E-11	1.3E-06	1.7E-06	1.3E-06	1.8E-06	5.4E-08	6.5E-09
CO	4.4E-05	2.5E-12	5.4E-05	5.6E-10	1.1E-05	2.6E-06	2.0E-09	1.0E-09	8.9E-10	2.9E-11
SIH	6.0E-11	2.4E-21	7.6E-11	2.7E-19	2.6E-10	1.4E-15	7.9E-19	4.3E-24	1.0E-25	4.3E-32
NO	3.4E-09	6.0E-17	4.6E-08	6.1E-15	1.1E-08	2.1E-13	2.9E-11	5.1E-13	1.3E-11	9.1E-16
O2	3.9E-07	7.0E-14	3.8E-06	5.0E-11	5.7E-06	3.0E-06	1.0E-11	2.0E-13	2.7E-12	2.1E-16
HS	5.2E-11	1.6E-13	2.5E-11	4.8E-13	8.2E-11	9.7E-13	9.7E-14	9.7E-13	1.1E-17	9.9E-19
SIC	8.5E-11	2.4E-11	1.0E-11	3.7E-11	2.1E-12	4.1E-11	6.3E-21	4.3E-11	3.7E-28	4.3E-11
SIO	1.9E-10	1.5E-11	2.9E-10	1.2E-10	3.1E-11	2.9E-10	9.0E-22	3.0E-10	4.6E-28	3.0E-10
CS	9.9E-10	9.4E-17	4.3E-09	2.3E-13	1.7E-09	2.3E-10	3.9E-14	1.1E-09	1.2E-16	4.1E-16
NS	1.5E-11	1.8E-14	7.2E-11	3.9E-13	1.1E-10	3.5E-12	6.3E-15	1.4E-12	2.2E-20	1.5E-18
SO	1.3E-10	1.2E-13	1.0E-09	1.0E-13	9.5E-10	2.6E-10	1.9E-16	1.2E-17	7.8E-20	4.8E-22

Table 8 – *continued*

t(yr)	1.0 x 10^5		3.2 x 10^5		1.0 x 10^6		1.0 x 10^7		1.0 x 10^8	
Species	Gas	Surface	Gas	Surface	Gas	Surface	Gas	Surface	Gas	Surface
SIS	1.9E-12	7.9E-14	5.3E-12	2.0E-12	1.1E-13	3.4E-12	1.7E-26	3.4E-12	8.0E-32	3.4E-12
S2	1.0E-15	3.0E-17	3.7E-15	1.2E-15	5.2E-16	2.6E-15	8.2E-22	3.0E-15	1.3E-22	3.0E-15
CH2	2.0E-07	1.8E-17	9.9E-08	8.1E-17	3.1E-08	3.0E-19	3.2E-09	3.2E-20	1.6E-09	3.0E-18
NH2	3.6E-08	8.5E-18	5.3E-07	8.4E-16	1.8E-06	1.2E-12	1.2E-06	1.8E-12	9.4E-08	1.1E-14
H2O	8.2E-08	8.4E-05	6.3E-07	1.8E-04	2.8E-07	2.4E-04	2.4E-09	2.6E-04	2.7E-09	2.6E-04
SIH2	1.5E-35	2.4E-21	2.9E-33	2.7E-19	6.9E-29	1.4E-15	1.1E-35	4.3E-24	5.1E-45	4.3E-32
MGH2	5.1E-40	4.1E-10	5.3E-39	2.2E-09	4.8E-38	8.0E-09	1.4E-37	1.4E-08	1.4E-37	1.4E-08
C2H	4.0E-08	1.6E-20	7.5E-09	3.3E-20	3.0E-09	6.6E-20	1.6E-10	6.8E-22	2.7E-11	2.4E-22
N2H	4.9E-18	4.5E-14	7.3E-16	2.8E-12	3.1E-13	2.6E-10	1.0E-12	4.8E-10	7.3E-14	3.3E-11
O2H	5.5E-24	7.4E-20	9.9E-21	5.3E-17	1.5E-15	2.0E-12	9.5E-18	3.4E-15	4.1E-25	2.0E-22
HS2	1.4E-14	3.1E-16	3.6E-13	6.5E-14	2.4E-13	4.1E-13	7.7E-20	5.6E-13	5.9E-22	5.6E-13
HCN	2.0E-08	1.3E-08	8.0E-08	1.0E-07	1.4E-07	5.9E-07	2.7E-09	1.2E-06	1.5E-10	1.9E-06
HNC	8.1E-09	4.6E-10	6.0E-08	2.2E-08	7.5E-08	1.4E-07	1.7E-09	3.1E-07	1.5E-10	5.9E-07
HCO	8.5E-13	9.6E-14	4.1E-12	5.7E-13	3.6E-10	5.8E-12	2.3E-12	1.6E-12	1.5E-12	1.5E-12
HOC	1.3E-23	4.2E-18	5.3E-21	9.3E-16	1.1E-16	4.4E-12	1.1E-19	1.7E-15	3.1E-21	4.8E-17
HCS	2.9E-29	2.9E-22	8.8E-26	7.0E-19	4.5E-22	7.0E-16	7.0E-21	3.4E-15	2.8E-27	1.2E-21
HNO	6.7E-11	2.7E-10	2.7E-10	1.2E-08	4.7E-11	6.3E-08	3.3E-12	6.7E-08	8.4E-16	9.6E-11
H2S	8.2E-12	2.0E-08	1.3E-10	6.0E-08	1.4E-10	1.2E-07	3.3E-13	1.2E-07	2.0E-17	1.2E-13
C3	3.2E-08	4.9E-21	3.4E-09	6.0E-21	6.0E-09	1.1E-20	1.2E-10	2.3E-22	5.7E-12	1.1E-23
O3	1.9E-29	8.1E-19	5.9E-24	7.5E-14	1.3E-17	2.2E-08	5.4E-23	3.2E-17	9.2E-28	6.0E-19
C2N	4.2E-09	6.9E-22	1.0E-08	2.8E-19	1.9E-09	1.3E-15	4.9E-12	6.2E-18	7.2E-14	6.7E-21
C2O	8.5E-37	2.0E-29	1.7E-33	6.1E-27	1.2E-31	8.4E-26	2.4E-35	1.3E-29	2.0E-34	1.0E-28
C2S	2.8E-10	4.3E-14	8.4E-11	1.5E-15	1.2E-11	9.7E-12	1.1E-16	3.8E-20	3.0E-20	1.7E-24
NAOH	1.1E-16	2.8E-18	1.6E-14	2.9E-15	4.5E-15	1.8E-14	1.2E-21	2.2E-14	9.8E-42	2.2E-14
OCN	7.5E-11	1.2E-23	5.6E-09	1.6E-19	5.6E-08	3.7E-14	9.3E-16	1.5E-15	6.2E-18	1.2E-18
CO2	1.3E-10	5.6E-11	6.3E-09	5.0E-09	7.9E-09	1.7E-08	6.6E-15	2.5E-08	6.2E-16	3.1E-08
OCS	3.6E-09	4.7E-22	2.6E-08	6.6E-19	2.3E-09	1.6E-15	2.8E-17	3.6E-17	3.4E-21	2.3E-22
SO2	4.6E-12	7.6E-11	1.2E-10	2.6E-09	9.1E-11	4.7E-09	1.0E-19	5.3E-09	1.0E-22	5.3E-09
CH3	3.6E-09	2.0E-17	4.4E-09	1.6E-16	3.9E-08	2.4E-16	2.8E-07	8.7E-16	1.1E-07	1.1E-14
NH3	8.2E-08	1.1E-05	1.3E-06	2.2E-05	2.5E-06	1.3E-05	1.4E-06	4.6E-06	1.1E-07	3.5E-07
SIH3	4.5E-37	2.4E-21	8.5E-35	2.7E-19	2.0E-30	1.4E-15	3.9E-37	4.3E-24	1.5E-46	4.3E-32
C2H2	1.5E-07	5.0E-14	3.5E-08	2.0E-12	7.8E-09	1.9E-08	2.6E-09	4.7E-09	2.8E-10	5.0E-11
N2H2	5.4E-12	1.2E-09	1.0E-09	7.5E-08	2.6E-07	6.9E-06	2.3E-07	1.3E-05	2.7E-09	8.8E-07
H2O2	1.1E-23	2.2E-13	2.0E-20	1.5E-10	1.2E-15	2.1E-06	2.9E-16	1.5E-07	8.3E-25	5.8E-16
H2S2	1.1E-15	2.3E-17	1.9E-14	4.1E-15	4.8E-15	1.4E-14	1.6E-21	1.8E-14	6.7E-23	1.8E-14
CH2N	9.6E-32	6.8E-27	1.6E-26	5.3E-22	4.3E-23	1.4E-19	2.7E-24	5.4E-21	2.1E-22	3.9E-19
CHNH	1.1E-27	4.5E-25	1.7E-25	1.8E-23	7.5E-26	4.5E-26	3.6E-27	5.3E-26	5.9E-24	8.5E-23
H2CO	1.3E-08	2.8E-06	6.1E-08	1.7E-05	3.2E-08	3.8E-05	6.6E-11	4.5E-05	6.3E-12	4.4E-05
CHOH	1.6E-24	4.2E-18	6.3E-22	9.3E-16	1.3E-17	4.4E-12	1.4E-20	1.7E-15	3.8E-22	4.8E-17
HCCN	9.0E-31	6.9E-22	1.2E-27	2.8E-19	2.2E-23	1.3E-15	3.0E-25	6.2E-18	3.4E-28	6.7E-21
HC2O	8.5E-37	2.0E-29	1.7E-33	6.1E-27	1.2E-31	8.4E-26	2.4E-35	1.3E-29	2.0E-34	1.0E-28
HNCO	3.3E-21	2.5E-12	3.2E-18	6.9E-10	1.1E-15	6.1E-08	5.1E-15	1.0E-07	8.8E-15	1.8E-07
C3H	9.4E-09	6.3E-21	4.2E-09	1.3E-20	1.0E-09	1.3E-20	7.0E-12	2.5E-22	2.8E-13	1.1E-23
H2CS	3.8E-11	4.0E-10	2.0E-10	5.4E-09	4.7E-11	9.5E-09	2.0E-14	2.8E-08	3.5E-17	1.5E-07
C4	3.0E-08	4.0E-21	2.1E-09	3.7E-21	1.6E-09	3.1E-21	2.0E-11	3.9E-23	2.0E-13	3.8E-25
C3N	1.0E-08	1.4E-21	1.0E-08	2.6E-19	9.8E-09	6.0E-15	3.3E-11	3.6E-17	5.1E-14	4.2E-21
C3O	1.2E-11	1.7E-24	1.4E-11	3.5E-22	1.8E-12	1.1E-18	4.5E-17	4.9E-23	1.2E-18	9.7E-26
C3S	1.2E-10	3.7E-11	3.7E-11	1.3E-10	4.6E-12	1.6E-10	7.0E-18	1.8E-10	4.0E-22	1.8E-10
CH4	1.9E-07	3.4E-05	1.3E-06	5.2E-05	8.8E-07	5.2E-05	5.4E-07	5.1E-05	1.1E-07	1.4E-05
SIH4	1.7E-26	2.2E-09	1.9E-25	7.3E-09	9.4E-25	1.4E-08	1.5E-24	1.6E-08	1.5E-24	1.6E-08
C2H3	1.1E-08	5.0E-20	1.4E-08	2.4E-18	7.7E-09	2.4E-14	2.3E-10	4.9E-15	2.6E-11	6.5E-17
CHNH2	2.0E-29	2.7E-25	3.2E-27	1.1E-23	4.5E-25	9.3E-22	4.6E-23	2.2E-20	2.9E-23	1.3E-20
CH2NH	2.6E-10	9.8E-12	1.4E-08	4.1E-09	9.0E-09	1.8E-08	1.2E-09	6.2E-08	2.5E-11	1.0E-07
CH3N	6.5E-33	7.7E-27	1.5E-27	1.1E-21	1.7E-21	1.1E-16	4.3E-21	1.5E-16	4.6E-20	1.4E-15
C3H2	1.0E-08	9.8E-15	5.0E-09	4.2E-13	1.3E-09	2.5E-09	9.0E-12	2.0E-10	3.5E-13	7.0E-13
CH2CN	3.6E-10	7.5E-22	4.5E-09	4.1E-19	1.5E-09	2.4E-15	6.0E-12	1.4E-17	8.1E-14	1.4E-20
CH2CO	1.8E-09	7.6E-11	4.0E-09	2.1E-09	1.3E-10	3.1E-09	2.1E-15	3.2E-09	1.0E-16	3.2E-09
HCOOH	2.0E-11	5.0E-13	1.1E-09	2.0E-10	2.5E-10	9.8E-10	2.6E-16	1.2E-09	2.2E-17	1.2E-09
CH2OH	4.1E-26	4.2E-18	1.6E-23	9.3E-16	3.5E-19	4.4E-12	3.7E-22	1.7E-15	1.0E-23	4.8E-17
NH2OH	1.0E-27	6.9E-16	1.8E-24	4.6E-13	3.0E-21	2.3E-10	7.1E-20	1.6E-09	7.2E-20	1.7E-09
C4H	3.3E-08	8.3E-21	7.6E-09	1.7E-20	5.4E-10	4.2E-21	2.1E-12	4.3E-23	1.6E-14	4.2E-25
HC3N	3.2E-09	2.3E-15	1.4E-08	7.2E-13	7.5E-09	5.2E-09	2.3E-11	7.5E-11	3.1E-14	8.0E-15
HC3O	4.5E-36	1.7E-24	2.4E-33	3.5E-22	3.3E-29	1.1E-18	4.4E-33	4.9E-23	8.8E-36	9.7E-26
C5	1.2E-08	1.4E-21	5.1E-10	8.9E-22	1.9E-10	3.6E-22	6.4E-13	1.2E-24	5.9E-16	1.1E-27
C4N	6.0E-10	3.1E-11	3.8E-10	2.7E-10	1.0E-10	4.0E-10	3.3E-16	6.0E-10	2.0E-21	6.0E-10
C4S	1.2E-11	4.0E-13	9.1E-12	6.1E-12	5.2E-13	7.5E-12	5.3E-19	7.9E-12	2.3E-24	7.9E-12
C2H4	4.9E-11	2.8E-15	1.8E-10	1.3E-13	2.2E-11	1.3E-09	2.2E-11	2.7E-10	1.5E-12	3.6E-12
CH2NH2	2.9E-31	2.7E-25	2.3E-28	1.1E-22	9.0E-23	1.3E-17	1.2E-22	3.7E-18	5.9E-24	1.8E-19
CH3NH	4.0E-30	2.4E-24	9.3E-25	3.2E-19	1.4E-20	6.1E-16	2.4E-20	3.9E-16	3.5E-19	5.3E-15

Table 8 – *continued*

t(yr)	1.0 x 10^5		3.2 x 10^5		1.0 x 10^6		1.0 x 10^7		1.0 x 10^8	
Species	Gas	Surface	Gas	Surface	Gas	Surface	Gas	Surface	Gas	Surface
CH3OH	1.5E-11	2.8E-06	3.2E-10	1.6E-05	3.3E-11	3.8E-05	6.6E-13	4.5E-05	1.0E-13	4.5E-05
C3H3	4.5E-12	8.6E-21	4.3E-11	3.7E-19	1.5E-11	2.2E-15	5.6E-13	1.9E-16	6.5E-15	7.0E-19
CH3CN	4.6E-11	2.0E-10	6.1E-10	6.5E-09	3.0E-10	1.5E-08	1.2E-12	1.8E-08	1.8E-14	1.9E-08
H2C3N	6.3E-35	1.9E-21	6.1E-32	6.1E-19	1.4E-27	4.4E-15	8.2E-29	6.3E-17	9.0E-33	6.8E-21
H2C3O	8.0E-26	7.5E-13	3.3E-24	7.5E-12	2.1E-23	1.4E-11	3.7E-23	1.5E-11	3.7E-23	1.5E-11
C4H2	1.1E-09	1.1E-14	7.1E-10	3.1E-13	8.2E-11	5.8E-10	4.8E-12	3.6E-11	1.3E-14	2.3E-14
C5H	4.1E-10	1.5E-21	1.2E-10	1.1E-21	1.1E-11	3.8E-22	1.2E-14	1.2E-24	6.7E-18	1.1E-27
C6	1.9E-09	2.1E-22	1.3E-10	2.2E-22	4.6E-11	8.5E-23	1.6E-14	3.0E-26	5.3E-18	9.9E-30
C5N	6.4E-10	7.5E-23	3.5E-10	7.1E-21	1.5E-10	7.5E-17	9.9E-14	9.0E-20	6.9E-18	4.6E-25
CH3NH2	2.0E-10	7.5E-12	1.0E-08	3.5E-09	6.0E-09	2.4E-08	7.6E-10	1.3E-06	1.6E-11	3.7E-05
C2H5	2.0E-27	7.5E-20	1.6E-25	2.5E-18	3.1E-21	2.3E-14	2.3E-21	4.9E-15	3.2E-23	6.6E-17
C3H4	9.0E-12	7.6E-09	1.1E-10	2.2E-08	3.3E-11	2.7E-08	1.4E-12	6.9E-08	1.5E-14	8.4E-08
C4H3	9.6E-34	9.2E-21	8.7E-32	2.6E-19	2.9E-28	4.9E-16	8.2E-29	3.1E-17	5.1E-32	1.9E-20
CH3CHO	1.3E-13	4.0E-15	1.2E-12	5.6E-13	7.9E-14	5.1E-12	3.8E-16	1.4E-10	1.2E-17	4.8E-08
H3C3N	7.2E-13	1.2E-16	4.9E-11	3.7E-14	8.4E-12	2.5E-10	6.7E-14	3.8E-12	5.8E-17	4.1E-16
C5H2	8.4E-11	1.9E-15	3.4E-10	2.7E-14	2.9E-11	5.1E-11	4.6E-14	8.8E-13	2.2E-17	5.6E-17
C6H	9.3E-11	2.2E-22	3.6E-11	2.8E-22	2.0E-12	8.9E-23	2.4E-16	3.1E-26	5.6E-20	1.0E-29
HC5N	8.9E-11	1.1E-16	2.8E-10	1.6E-14	3.7E-11	4.5E-11	1.4E-14	1.4E-13	4.9E-19	6.2E-19
C7	4.5E-10	4.6E-23	3.8E-11	6.2E-23	8.2E-12	1.5E-23	8.9E-16	1.6E-27	6.9E-20	1.2E-31
H4C3N	1.0E-37	1.9E-21	1.0E-34	6.1E-19	2.1E-30	4.1E-15	1.4E-31	6.3E-17	1.5E-35	6.8E-21
CH3C3N	1.4E-12	2.8E-14	2.5E-11	8.6E-12	3.1E-12	1.4E-11	1.9E-15	1.7E-11	6.7E-19	1.7E-11
H2C5N	9.3E-44	8.6E-23	4.7E-41	1.3E-20	3.4E-37	3.6E-17	6.5E-39	1.1E-19	2.4E-44	5.0E-25
C2H6	6.4E-17	3.4E-08	9.0E-16	1.3E-07	3.2E-15	1.7E-07	9.9E-15	4.1E-07	2.1E-14	8.6E-07
C4H4	3.2E-23	7.0E-09	4.1E-22	2.2E-08	1.3E-21	2.4E-08	2.7E-21	3.6E-08	2.8E-21	3.7E-08
C5H3	4.2E-40	1.6E-21	1.8E-38	2.2E-20	5.5E-35	4.2E-17	5.4E-36	7.2E-19	3.2E-40	4.6E-23
C6H2	3.5E-10	3.5E-16	9.4E-11	6.6E-15	2.9E-12	9.7E-12	5.6E-15	2.9E-14	1.4E-18	5.7E-19
C7H	2.5E-11	4.9E-23	1.3E-11	8.3E-23	3.7E-13	1.5E-23	1.3E-17	1.6E-27	7.0E-22	1.3E-31
C8	1.6E-10	1.5E-23	1.2E-11	1.9E-23	1.5E-12	2.6E-24	1.2E-16	2.1E-28	2.4E-21	4.2E-33
C7N	3.8E-11	3.8E-24	3.7E-11	6.6E-22	3.8E-12	1.7E-18	6.4E-17	5.0E-23	2.5E-22	1.5E-29
CH3OCH3	6.0E-16	1.3E-17	7.1E-14	1.7E-14	1.6E-15	3.0E-14	5.9E-18	3.2E-14	2.6E-19	3.2E-14
C2H5OH	3.0E-15	5.6E-17	3.2E-13	7.8E-14	1.4E-14	2.9E-12	1.5E-16	1.9E-11	3.6E-18	3.8E-11
CH3C4H	3.9E-11	9.3E-13	3.3E-10	1.1E-10	1.9E-11	1.7E-10	4.2E-14	2.1E-10	1.7E-17	2.1E-10
C5H4	7.1E-29	1.5E-09	6.5E-28	3.2E-09	1.9E-27	3.4E-09	3.5E-27	4.4E-09	3.5E-27	4.4E-09
C6H3	1.8E-43	2.8E-22	1.6E-41	5.3E-21	3.1E-38	7.8E-18	1.0E-39	2.4E-20	1.1E-44	4.6E-25
C7H2	2.5E-11	6.9E-17	2.0E-11	1.7E-15	5.3E-13	1.6E-12	2.4E-17	1.8E-15	9.3E-22	5.6E-21
C8H	3.5E-11	1.8E-23	6.9E-12	3.0E-23	9.2E-14	2.8E-24	2.0E-18	2.1E-28	3.5E-23	4.3E-33
HC7N	8.3E-12	5.9E-18	3.9E-11	1.7E-15	2.8E-12	1.3E-12	4.7E-17	2.8E-16	1.6E-22	3.1E-23
C9	3.6E-11	3.2E-24	2.0E-12	3.1E-24	1.7E-13	3.0E-25	2.4E-18	4.1E-30	4.8E-24	8.2E-36
H3C5N	1.5E-33	3.4E-11	7.7E-32	3.8E-10	4.2E-31	5.1E-10	1.1E-30	8.6E-10	1.1E-30	8.6E-10
H5C3N	5.5E-27	6.4E-10	4.6E-25	1.1E-08	3.5E-24	2.3E-08	1.5E-23	5.8E-08	1.5E-23	6.0E-08
CH3C5N	2.9E-14	5.1E-16	3.7E-13	1.5E-13	1.3E-14	1.9E-13	9.8E-19	2.0E-13	9.3E-24	2.0E-13
H2C7N	1.1E-52	4.7E-24	1.9E-49	1.4E-21	3.1E-46	1.1E-18	2.8E-48	2.2E-22	4.2E-56	2.4E-29
C6H4	2.1E-32	1.7E-10	3.5E-31	6.2E-10	1.2E-30	6.5E-10	2.3E-30	8.6E-10	2.3E-30	8.6E-10
C7H3	3.4E-49	5.5E-23	4.5E-47	1.3E-21	5.7E-44	1.3E-18	1.8E-45	1.4E-21	1.2E-51	4.4E-27
C8H2	5.7E-12	2.6E-17	3.9E-12	5.2E-16	4.8E-14	2.6E-13	8.0E-18	4.3E-16	4.6E-23	1.9E-22
C9H	6.7E-13	3.3E-24	6.1E-13	4.1E-24	8.6E-15	3.1E-25	3.9E-20	4.2E-30	4.3E-26	8.3E-36
C9N	1.8E-12	1.6E-25	1.3E-12	2.1E-23	4.3E-14	1.7E-20	6.9E-20	4.9E-26	6.7E-27	3.5E-34
CH3C6H	1.4E-13	2.3E-15	2.3E-12	6.7E-13	9.9E-14	9.5E-13	6.8E-18	1.1E-12	1.1E-22	1.1E-12
C7H4	2.3E-38	2.4E-11	6.4E-37	1.3E-10	2.4E-36	1.4E-10	4.6E-36	1.7E-10	4.6E-36	1.7E-10
C8H3	3.0E-52	2.0E-23	4.8E-50	4.1E-22	2.5E-47	2.1E-19	2.2E-48	3.4E-22	1.2E-55	1.5E-28
C9H2	4.3E-13	4.5E-18	1.3E-12	8.6E-17	1.3E-14	2.9E-14	7.8E-20	2.1E-17	7.6E-26	3.5E-25
HC9N	2.7E-13	2.4E-19	1.5E-12	5.8E-17	3.5E-14	1.4E-14	5.5E-20	2.0E-18	4.6E-27	7.6E-28
H3C7N	8.6E-43	1.0E-12	2.6E-40	4.4E-11	1.5E-39	5.2E-11	2.9E-39	6.1E-11	2.9E-39	6.1E-11
CH3C7N	2.5E-15	2.9E-17	5.2E-14	2.3E-14	9.1E-16	2.6E-14	3.2E-21	2.7E-14	3.0E-27	2.7E-14
H2C9N	1.5E-61	1.8E-25	2.3E-58	4.5E-23	1.2E-55	1.1E-20	1.9E-57	1.6E-24	4.2E-68	5.9E-34
C8H4	1.4E-41	6.2E-12	8.2E-40	5.1E-11	3.2E-39	5.3E-11	5.9E-39	6.1E-11	5.9E-39	6.1E-11
C9H3	5.9E-58	3.6E-24	8.2E-56	6.7E-23	3.1E-53	2.3E-20	2.0E-54	1.6E-23	2.7E-63	2.8E-31
C9H4	2.7E-47	1.1E-12	1.4E-45	8.2E-12	5.7E-45	8.4E-12	1.0E-44	9.1E-12	1.0E-44	9.1E-12
H3C9N	8.9E-52	3.7E-14	2.8E-49	1.6E-12	1.6E-48	1.8E-12	3.0E-48	1.9E-12	3.0E-48	1.9E-12
E	8.8E-08		3.5E-08		3.0E-08		3.5E-08		1.5E-07	
H+	2.4E-08		6.5E-10		1.7E-10		4.0E-10		7.2E-09	
HE+	1.1E-09		7.1E-10		1.0E-09		2.7E-09		1.0E-08	
C+	3.1E-08		2.3E-09		5.1E-10		1.5E-11		9.7E-11	
N+	1.5E-11		3.0E-11		1.2E-10		1.9E-10		6.5E-11	
O+	4.4E-15		5.0E-15		7.2E-15		1.2E-16		7.1E-16	
NA+	3.5E-09		2.5E-09		1.1E-09		1.0E-13		1.5E-32	
MG+	1.2E-08		7.9E-09		3.1E-09		1.6E-13		8.3E-35	
SI+	6.8E-10		1.2E-11		1.7E-12		3.0E-20		2.1E-26	
S+	3.0E-09		4.7E-11		4.1E-12		1.4E-15		9.4E-17	

Table 8 – *continued*

t(yr)	1.0 x 10^5		3.2 x 10^5		1.0 x 10^6		1.0 x 10^7		1.0 x 10^8	
Species	Gas	Surface	Gas	Surface	Gas	Surface	Gas	Surface	Gas	Surface
FE+	5.8E-09		4.8E-09		3.6E-09		6.2E-10		1.2E-12	
O2+	1.1E-10		6.3E-11		3.4E-11		1.3E-16		1.4E-16	
CH+	1.4E-13		3.0E-14		6.4E-15		1.6E-15		2.0E-15	
SO+	2.0E-11		9.5E-12		9.6E-13		1.5E-18		3.4E-20	
H3+	1.4E-09		3.3E-09		6.4E-09		1.9E-08		1.3E-07	
CH2+	3.6E-13		5.0E-14		1.2E-14		5.7E-15		9.6E-15	
NH2+	5.1E-13		3.8E-13		9.2E-13		1.4E-12		8.5E-13	
HCO+	1.5E-09		5.2E-09		1.9E-09		1.2E-12		1.1E-12	
HOC+	1.5E-10		4.5E-10		1.9E-10		8.5E-14		6.6E-14	
N2H+	1.3E-13		1.1E-11		1.1E-10		3.5E-10		2.4E-11	
C2N+	3.6E-10		3.1E-10		1.2E-10		7.9E-14		6.3E-15	
HCS+	3.6E-11		2.6E-11		3.6E-11		2.1E-15		1.0E-17	
OCS+	1.5E-10		5.6E-11		2.3E-12		3.7E-20		4.1E-23	
H3O+	5.9E-10		1.3E-09		4.6E-10		1.1E-11		2.7E-11	
HCO2+	1.8E-14		3.2E-13		7.6E-13		1.8E-18		2.6E-19	
H2CN+	1.0E-10		7.3E-10		1.2E-09		5.9E-11		7.8E-12	
CH3+	3.0E-10		8.4E-11		2.2E-11		1.2E-11		2.2E-11	
NH3+	6.2E-11		7.2E-11		1.9E-10		2.9E-10		1.5E-10	
CH4+	1.0E-14		1.4E-15		8.0E-16		1.2E-14		3.4E-14	
NH4+	3.9E-10		3.0E-09		9.1E-09		1.1E-08		1.3E-09	
CH5+	1.6E-10		1.9E-10		1.4E-10		3.0E-10		1.6E-10	
C2H2+	1.6E-10		9.7E-12		4.0E-12		2.5E-13		1.9E-13	
C2H3+	7.1E-11		4.5E-11		8.5E-12		2.6E-12		5.7E-13	
C2H4+	1.9E-10		7.5E-11		5.6E-11		3.5E-12		6.0E-13	
C3H3+	3.8E-10		6.0E-11		2.0E-11		2.8E-13		1.8E-14	
C3H2N+	1.2E-10		2.6E-10		2.2E-10		1.6E-12		3.4E-15	
CH4N+	2.2E-12		5.1E-11		4.6E-11		1.3E-11		4.6E-13	
CH6N+	3.4E-12		5.4E-11		3.8E-11		1.0E-11		3.3E-13	
GRAIN0	2.9E-14		1.4E-14		1.4E-14		2.4E-14		3.8E-14	
GRAIN-	2.6E-12		2.6E-12		2.6E-12		2.6E-12		2.6E-12	

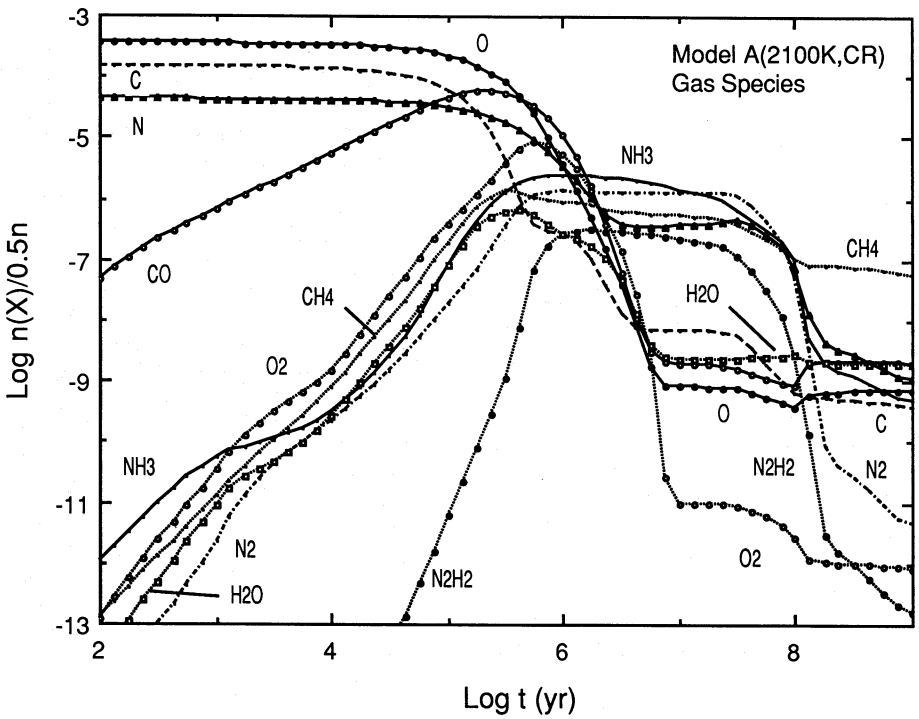

Figure 2. Fractional abundances (with respect to $n/2$) of selected small molecules in the gas phase are depicted as functions of time for model A(2100K, CR).

abundances of their unsaturated counterparts (e.g. NH_2, CH_3). The quasi-steady state is maintained up to 10^8 yr via the following processes: (i) destruction of saturated gas-phase molecules (e.g. CH_4, N_2H_2, NH_3) by abundant ions followed by rapid dissociative recombination reactions leading to the production of other neutral species, and (ii) accretion and surface hydrogenation followed by desorption of easily desorbed species. During the repeated cycles, carbon and nitrogen are removed gradually from the cycle and converted into surface CH_3NH_2, which desorbs slowly and achieves a large surface abundance. Methyl amine is formed via surface reactions between reactive and mobile CH_3 and NH_2 radicals deposited from the gas. By 10^8 yr, the available nitrogen for this cycle, which is smaller than the available carbon in this model, is exhausted. The gaseous nitrogen-containing molecules sink to lower abundances, whereas methane and CH_3 maintain their high gaseous abundances. Interestingly, this behaviour is in contrast to that observed in model N(2100K, CR), in which the total volatile carbon in the late-stage gas-surface cycle is lower than the total volatile nitrogen, so that it is the nitrogen-containing molecules that maintain large gas-phase abundances at times until 10^8 yr.

As for complex organic molecules, by a time of 10^7 yr they have been slowly hydrogenated on grain surfaces to the most saturated forms in the model. These saturated surface species generally show little time dependence in their abundances at times later than 1×10^6 yr, having been produced via gas-phase syntheses of precursor unsaturated molecules. For example, the fractional abundance of C_9H_4 stays fixed at $\approx10^{-11}$ and that of H_3C_9N stays fixed at $\approx10^{-12}$. These values are lower than achieved in models N(2100K) and N(2110K, CR) due to less efficient gas-phase syntheses of precursor unsaturated species. One complex molecule that does reach high surface abundances at late times in model A(2100K, CR) is methyl amine (CH_3NH_2), as discussed above.

6 CONCLUSIONS

There are two major conclusions of this paper. First, the synthesis of complex molecules on 10-K grain surfaces does not proceed, even for models that are poor in atomic H and rich in H_2, if the activation energy of reactions of hydrocarbon radicals C_n and C_nH with H_2 is 2100 K. Such a low activation energy allows tunnelling to take place and produce more saturated, less reactive molecular species. In this case, complex organic molecules can only be produced in the gas. This conclusion is important, given the large uncertainties in the gas-phase abundances of complex molecules and the search for alternative synthetic pathways. Quantum chemical studies to determine the actual activation energies are urgently needed. We are currently investigating the possibility that, at higher grain temperatures, which pertain to star formation regions if not quiescent sources, H_2 is desorbed so rapidly from grains that it cannot hydrogenate reactive radicals. If this hypothesis is correct, grain synthesis of complex species might occur on warmer grains more efficiently.

Our second major conclusion is that cosmic ray induced desorption processes cannot prevent the bulk of the heavy gaseous material from accreting on to dust particles in sufficiently long times if the overall gas density n is 2×10^4 cm^{-3}. This is especially true for water ice and the larger, more complex species, which tend to have larger grain adsorption energies E_D. In all of our models, the final disposition of complex molecules is that they tend to be hydrogenated to the limits allowed in the calculations and to reside on grain surfaces. These 'dirty (organic) snowball' results should be of interest to those investigators studying relatively pristine Solar System objects such as comets and parts of meteors. For lower gas densities than considered here, it has been suggested that significant gas-phase abundances of CO (Léger et al. 1985) and H_2CO (Federman & Allen 1991) can possibly be maintained in the gas for arbitrarily long periods of time via cosmic ray induced desorption or, in the case of H_2CO, other desorption processes. Model results for a model of the type N(2100K, CR) run at a gas density $n=2\times10^3$ cm^{-3} show a complicated picture. At times until 10^7 yr, large abundances of CO and H_2CO remain in the gas due mainly to the slowness of accretion at the low gas and dust densities. At later times, desorption helps to maintain non-negligible fractional abundances of these species in the gas, but the fractional abundances – 10^{-8} and 10^{-11} for CO and H_2CO respectively – are significantly below observed values.

We have run a variety of time-dependent models, both with and without cosmic ray induced desorption, at $n=2\times10^4$ cm^{-3} and $T=10$ K, and present a large body of gas-phase and surface fractional abundances as a function of time. A previous model with which some of our results for smaller molecules can be compared is the gas–grain model of d'Hendecourt et al. (1985). These authors considered non-thermal desorption to occur mainly via ultraviolet-catalysed and collision-induced grain explosions, at a rate *uniform* for all species in the model. Comparison with their results is hindered by the fact that the physical conditions of their models do not coincide with ours. Their 'standard' model, with density, temperature, and initial abundances similar to our model A(2100K, CR), contains a low value for the visual extinction ($A_V=4$ mag) which causes a true steady state to exist at times between 10^7 and 10^8 yr. Perhaps a better comparison is afforded between our A(2100K, CR) model and their high-density, high-extinction model ($n=10^5$ cm^{-3}, $A_V=8$ mag), although their density is an order of magnitude higher than ours. In their model, a true steady state is also not reached at late stages. Detailed comparison at 10^7 yr shows good agreement between the two models for H_2O, CH_4, NH_3 and N_2 surface abundances, and for N_2 and to a lesser extent NH_3 gaseous abundances. Strong disagreements for other species (CO, CO_2, O_2) arise from our inclusion of surface hydrogenation of O_2, our difficulty in desorbing H_2O from grain surfaces, and their efficient conversion of surface CO to surface CO_2. In general, these differences reflect continuing uncertainties in our understanding of surface chemical rates and non-thermal desorption mechanisms.

It is also natural to inquire about the agreement between our results and observation. We can compare our surface chemical results with limited observations in quiescent interstellar sources, especially the results concerning surface CO and H_2O in the Taurus region summarized by Whittet & Duley (1991). In addition to these results, the recent surface observation of CH_4 (Lacy et al. 1991) in the relatively quiescent gas in front of 7538 IRS 9 should be reproducible by our model calculations. These observations are listed in

Table 9. Comparison with surface observations of quiescent regions.

	$n_s(CO)/n(CO)$	$n_s(CO)/n(H_2)$	$n_s(CO)/n_s(H_2O)$	$n_s(CH_4)/n_s(CO)$
Observations				
Taurus[a]	0.25	2.9 (-5)	0.2	---
7538IRS9[b]	0.10	---	0.24	0.13
Model N(2100K)				
1 x 10^5 yr	0.037	2.5 (-6)	0.050	0.25
3 x 10^5 yr	0.15	8.9 (-6)	0.081	0.21
1 x 10^6 yr	0.64	8.3 (-6)	0.049	0.32
1 x 10^7 yr	6.5 (+7)	1.7 (-17)	8.5 (-14)	2.2 (+11)
Model N(2100K,CR)				
1 x 10^5 yr	0.037	2.5 (-6)	0.050	0.25
3 x 10^5 yr	0.14	8.6 (-6)	0.078	0.22
1 x 10^6 yr	0.53	7.4 (-6)	0.044	0.35
1 x 10^7 yr	0.44	4.8 (-10)	2.4 (-6)	7.9 (+3)
1 x 10^8 yr	0.34	3.4 (-10)	1.7 (-6)	1.1 (+4)

Note: $a(-b)$ represents $a \times 10^{-b}$. [a]Whittet & Duley (1991); see discussion in HHL; [b]Lacy et al. (1991) and Mitchell et al. (1990).

Table 9, which is similar to table 10 of HHL, in the form of abundance ratios $n_s(CO)/n(CO)$, $n_s(CO)/n(H_2)$, $n_s(CO)/n_s(H_2O)$ and $n_s(CH_4)/n_s(CO)$. As shown in HHL, only models with normal initial conditions need be considered because models with atomic initial conditions dramatically underproduce surface CO, both at early times, when surface C and O are hydrogenated before they can stick together, and at later times, when slow hydrogenation to formaldehyde and methanol is the rule for all of our models.

HHL showed that their model D (normal initial conditions) was in good agreement with surface observations at times from 10^5 to 10^6 yr. The same can be said about our new models N(2100K) and N(2100K, CR), the results of which for the four abundance ratios are listed in Table 9 from 10^5 to 10^8 yr. Clearly, the lower activation energy for reactions of types (4) and (5) does not affect the limited results shown, nor, for $t \leq 10^6$ yr, does the existence of cosmic ray induced desorption. While it is true that the presence of cosmic ray induced desorption does increase the surface CO abundance at times greater than 10^6 yr by preventing all of it from being hydrogenated, as discussed in Section 5.1, the calculated abundances are still much lower than observed. We plan in future to consider striated grains in which molecules such as CO lying deep inside mantles are less reactive than those lying near the surface. With such grains, it is expected that agreement with mantle observations can be obtained for times later than is currently possible. Observations of complex gas-phase molecules in quiescent sources, however, still appear to be accounted for best by gas-phase syntheses at early times.

ACKNOWLEDGMENTS

EH acknowledges the support of the National Science Foundation for his research programme in astrochemistry. He also wishes to thank the Ohio Supercomputer Center for computer time on their Cray Y-MP/8, and the North Carolina Supercomputing Center for computer time on their Cray Y-MP/4, where much of the necessary computing was performed.

REFERENCES

Allen M., Robinson G. W., 1977, ApJ, 212, 396
Baldwin R. R., Walker R. W., Langford D. H., 1969, Trans. Faraday Soc., 65, 2116
Baulch D. L., Cox R. A., Hampson R. F., Jr, Kerr J. A., Troe J., Watson R. T., 1984, J. Phys. Chem. Ref. Data, 13, 1259
Blake G. A., Sutton E. C., Masson C. R., Phillips T. G., 1987, ApJ, 315, 621
Brown P. D., 1990, MNRAS, 243, 65
Brown P. D., Charnley S. B., 1990, MNRAS, 244, 432
d'Hendecourt L. B., Allamandola L. J., Greenberg J. M., 1985, A&A, 152, 130
Federman S. R., Allen M., 1991, ApJ, 375, 157
Graedel T. E., Langer W. D., Frerking M. A., 1982, ApJS, 48, 321
Grim R. J. A., d'Hendecourt L. B., 1986, A&A, 167, 161
Hasegawa T. I., Herbst E., Leung C. M., 1992, ApJS, 82, 167 (HHL)
Herbst E., Leung C. M., 1989, ApJS, 69, 271
Herbst E., Leung C. M., 1990, A&A, 233, 177
Herbst E., DeFrees D. J., Talbi D., Pauzat F., Koch W., McLean A. D., 1991, J. Chem. Phys., 94, 7842
Iglesias E. R., Silk J., 1978, ApJ, 226, 851
Kurylo M. J., Timmons R. B., 1969, J. Chem. Phys., 50, 5076
Lacy J. H., Carr J. S., Evans N. J., II, Baas F., Achtermann J. M., Arens J. F., 1991, ApJ, 376, 556
Léger A., Jura M., Omont A., 1985, A&A, 144, 147
Leung C. M., Herbst E., Huebner W. F., 1984, ApJS, 56, 231
Millar T. J., Herbst E., 1990, A&A, 231, 466
Mitchell G. F., 1984a, ApJS, 54, 81
Mitchell G. F., 1984b, ApJ, 287, 665
Mitchell G. F., Deveau T. J., 1983, ApJ, 266, 646

Mitchell G. F., Maillard J.-P., Allen M., Beer R., Belcourt K., 1990, ApJ, 363, 554
Pickles J. B., Williams D. A., 1977a, A&SS, 52, 443
Pickles J. B., Williams D. A., 1977b, A&SS, 52, 453
Smith I. M. W., 1988, in Millar T. J., Williams D. A., eds, Rate Coefficients in Astrochemistry. Kluwer, Dordrecht, p. 103
Tielens A. G. G. M., Allamandola L. J., 1987, in Hollenbach D. J., Thronson H. A., Jr, eds, Interstellar Processes. Kluwer, Dordrecht, p. 397
Tielens A. G. G. M., Hagen W., 1982, A&A, 114, 245
Watson W. D., 1975, in Balian et al., eds, Atomic and Molecular Physics and the Interstellar Matter. Les Houches Summer School, Session XXVI, North-Holland, Amsterdam, p.181
Watson W. D., 1976, Rev. Mod. Phys., 48, 513
Westley F., 1980, Table of Recommended Rate Constants for Chemical Reactions Occurring in Combustion. NSRDS-NBS67, Washington, D.C.
Whittet D. C. B., Duley W. W., 1991, Astr. Astrophys. Rev., 2, 167
Williams D. A., Millar T. J., eds., 1992, Dust and Chemistry in Astronomy. Hilger, Bristol, in press